

# Perfect matchings of trimmed Aztec rectangles

Tri Lai

University of Nebraska - Lincoln  
Lincoln, NE 68588 USA

tlai3@unl.edu

Submitted: Sep 6, 2016; Accepted: Oct 3, 2017; Published: Oct 20, 2017

Mathematics Subject Classifications: 05A15, 05B45, 05C30

## Abstract

We consider several new families of subgraphs of the square grid whose matchings are enumerated by powers of several small prime numbers: 2, 3, 5, and 11. Our graphs are obtained by trimming two opposite corners of an Aztec rectangle. The result yields a proof of a conjecture posed by Ciucu. In addition, we reveal a hidden connection between our graphs and the hexagonal dungeons introduced by Blum.

**Keywords:** perfect matching, tiling, dual graph, Aztec rectangle, graphical condensation, hexagonal dungeon.

## 1 Introduction and main results

A *perfect matching* of a graph  $G$  is a collection of edges of  $G$  so that each vertex is covered by precisely one edge in the collection. A perfect matching is sometimes called 1-factor (in graph theory) or dimmer covering (in statistical mechanics). The field of enumeration of perfect matchings date back to the early 1960's when Kasteleyn [8] and Temperley and Fisher [29] found the number of tilings of a rectangle on the square grid. In 1992, Elkies, Kuperberg, Larsen, and Propp [6, 7] proved a striking pattern for the number of perfect matchings of an *Aztec diamond graph* (see the definition below), which is a power of 2. This result opened two-and-a-half flourishing decades of the enumeration of perfect matchings.

Consider a  $\sqrt{2}m \times \sqrt{2}n$  rectangular contour rotated  $45^\circ$  and translated so that its vertices are centers of unit squares on the square grid (see the dotted contour on the left picture of Figure 1.1). The  $m \times n$  *Aztec rectangle (graph)*<sup>1</sup>  $AR_{m,n}$  is the subgraph of the square grid induced by the vertices inside or on the boundary of the rectangular contour (see the graph restricted by the left bold contour in Figure 1.1 for the Aztec rectangle  $AR_{6,8}$ ). The Aztec rectangle  $AR_{m,n}$  is called the *Aztec diamond* of order  $n$  when  $m = n$ .

---

<sup>1</sup>From now on, the term “Aztec rectangle” will be used to mean “Aztec rectangle graph”.

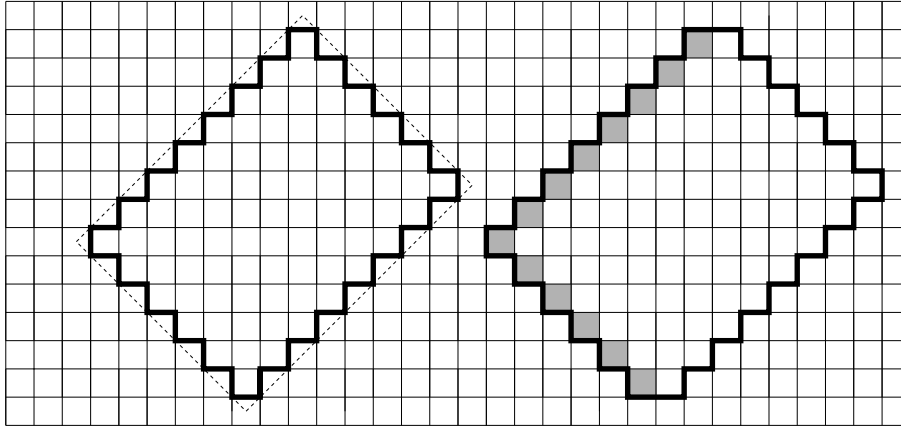


Figure 1.1: The Aztec rectangle  $AR_{6,8}$  (left) and the augmented Aztec rectangle  $AA_{6,8}$  (right).

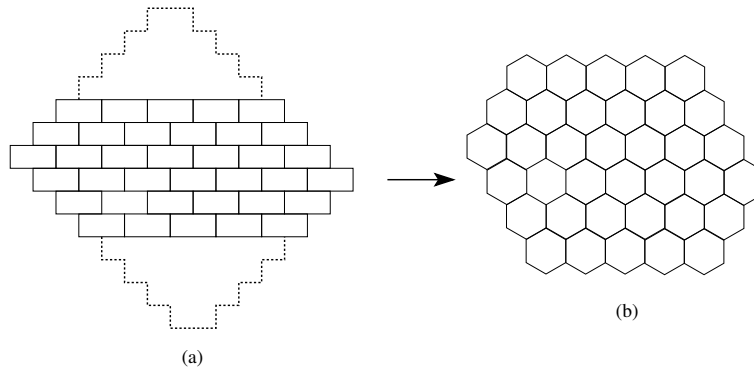


Figure 1.2: Obtaining a honeycomb graph from a trimmed augmented Aztec rectangle on the brick lattice.

The *augmented Aztec rectangle*  $AA_{m,n}$  is obtained by stretching the Aztec rectangle  $AR_{m,n}$  one unit horizontally, i.e. adding one square to the left of each row in the Aztec rectangle (see the graph restricted by the black contour on the right of Figure 1.1; the added squares are shaded ones). We can still define the Aztec rectangle and augmented Aztec rectangle on sub-grids or weighted versions of the square grid. The graph  $AA_{n,n}$  is called the *augmented Aztec diamond* of order  $n$ .

It has been shown in [6, 7] that the Aztec diamond of order  $n$  (i.e. the Aztec rectangle  $AR_{n,n}$ ) has  $2^{n(n+1)/2}$  perfect matchings, and it is easy to see that  $AR_{m,n}$  has no perfect matching when  $m \neq n$ . Sachs and Zernitz [26] proved that the augmented Aztec diamond of order  $n$  has  $D(n, n)$  perfect matchings, where the *Delannoy number*  $D(m, n)$ , for  $m, n \geq 0$ , is the number of lattice paths on  $\mathbb{Z}^2$  from the vertex  $(0, 0)$  to the vertex  $(m, n)$  using north, northeast and east steps (see e.g. Exercise 6.49 in [28]). Dana Randall later gave a simple combinatorial proof for the result. More general, the number of perfect matchings of the augmented Aztec rectangle  $AA_{m,n}$  is given by the  $D(m, n)$ , for any  $m, n$ .

Various families of subgraphs of the square grid have been investigated, focusing on

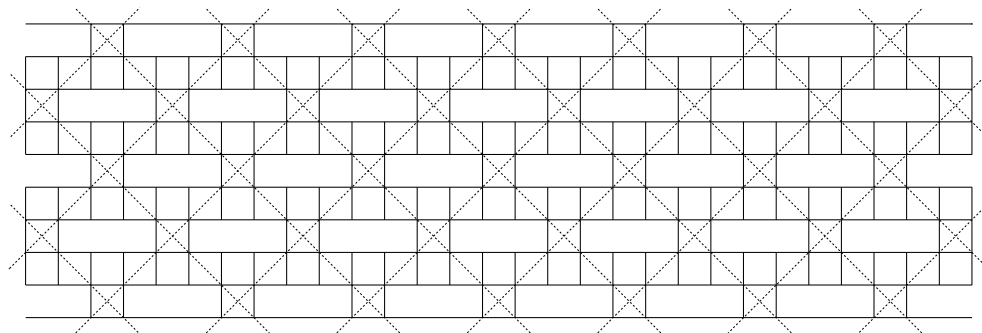


Figure 1.3: The  $B$  lattice (solid lines), and its partition into crosses (restricted by dotted diamonds).

the ones having perfect matchings enumerated by perfect powers (see e.g., [1], [6], [13], [23], [30], and the references therein). However, in most cases, the graphs are either highly symmetric or some variants of the Aztec rectangles. In this paper, we introduced six new families of subgraphs that are *not* Aztec-rectangle-like. However, their perfect matchings are still enumerated by perfect powers (see the graphs  $A_{a,b,c}^{(i)}$  and  $F_{a,b,c}^{(i)}$ , for  $i = 1, 2, 3$ , in Section 2).

Here is a simple observation that inspires our main results. Viewing a standard brick lattice as a sub-grid of the square grid, we consider an augmented Aztec rectangle on the standard brick lattice, where the north and the south corners have been trimmed (see Figure 1.2(a)). One readily sees that the resulting graph can be deformed into the honeycomb graph whose perfect matchings are enumerated by MacMahon's formula [10] (see Figure 1.2(b)).

Next, we consider a new brick lattice  $B$  pictured in Figure 1.3. In particular, the lattice  $B$  is obtained by gluing copies of a cross pattern, which is restricted in a dotted diamond of side  $2\sqrt{2}$ . Let  $a$  and  $b$  be two non-negative integers. Consider a  $(2b+2a-2) \times (2b+4a-2)$  augmented Aztec rectangle on the new lattice so that its east corner is the east corner of a cross pattern. Similar to the case of the standard brick lattice, we trim the north and south corners of the augmented Aztec rectangle both from right to left at levels  $(2a-1)$  above and  $(4a-1)$  below the eastern corner, respectively. The only difference here is that we are using two zigzag cuts containing alternatively "bumps" and "holes" of size 2, as opposed to straight cuts in the case of standard brick lattice (see Figure 1.4). Denote by  $TR_{a,b}$  the resulting graph. The number of perfect matchings of  $TR_{a,b}$  is given by the theorem stated below.

**Theorem 1.1.** *Assume that  $a$  and  $b$  are positive integers so that  $b \geq 2a$ . Then the number of perfect matchings of  $TR_{a,b}$  is  $10^{8k^2} 11^{2k^2}$  if  $a = 2k$ , and  $10^{2(2k+1)^2} 11^{2k(k+1)}$  if  $a = 2k+1$ .*

We note that the number of perfect matchings of  $TR_{a,b}$  in Theorem 1.1 does *not* depend on  $b$ .

We now consider a  $2m \times 2n$  Aztec rectangle ( $m \leq n$ ) on the lattice  $B$  whose east corner is also the east corner of a cross pattern. Similar to the graph  $TR_{a,b}$ , we also trim

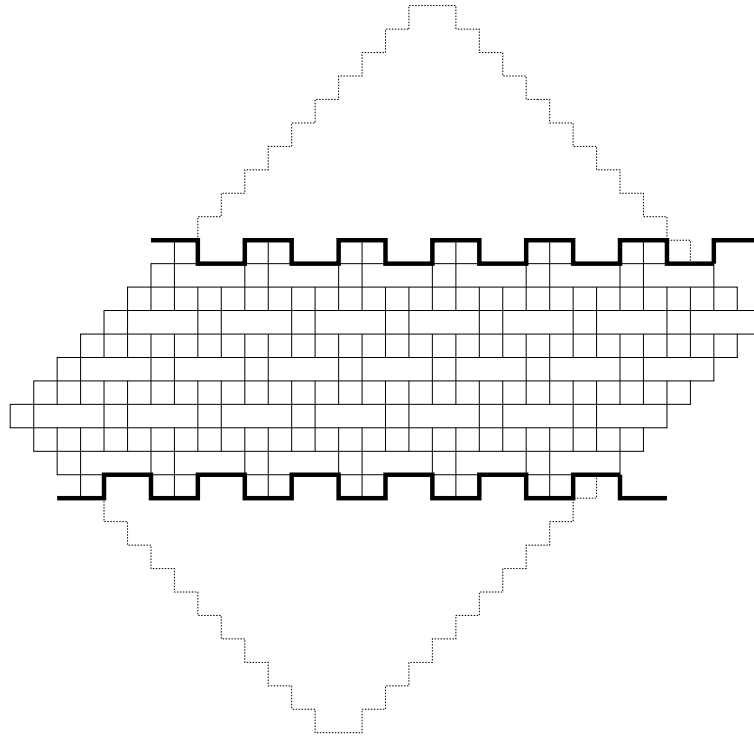


Figure 1.4: The trimmed augmented Aztec rectangle  $TR_{2,6}$  on the lattice  $B$ .

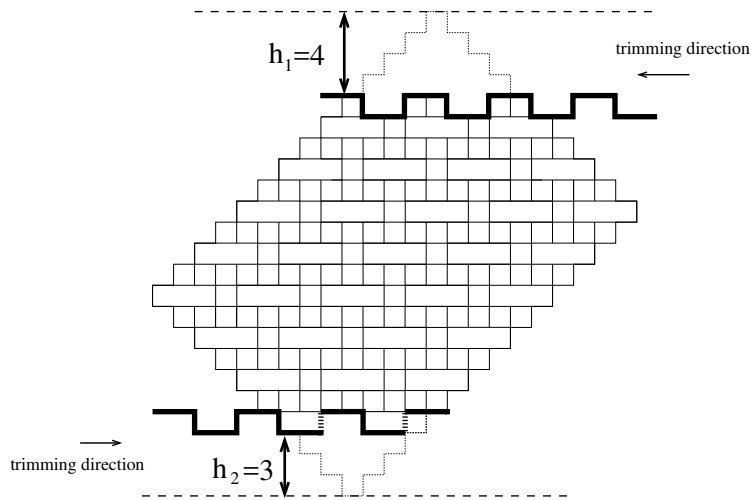


Figure 1.5: The graph  $TA_{5,7}^{4,3}$  is obtained by trimming the rectangle  $AR_{10,14}$  (on the lattice  $B$ ) by two zigzag cuts.

the upper and lower corners of the Aztec rectangle by two zigzag cuts. The only difference here is that we are trimming the north corner from right to left and the south corner from left to right. Assume that  $h_1$  is the distance between the top of the Aztec rectangle and the upper cut, and that  $h_2$  is the distance between the bottom of the graph and the lower

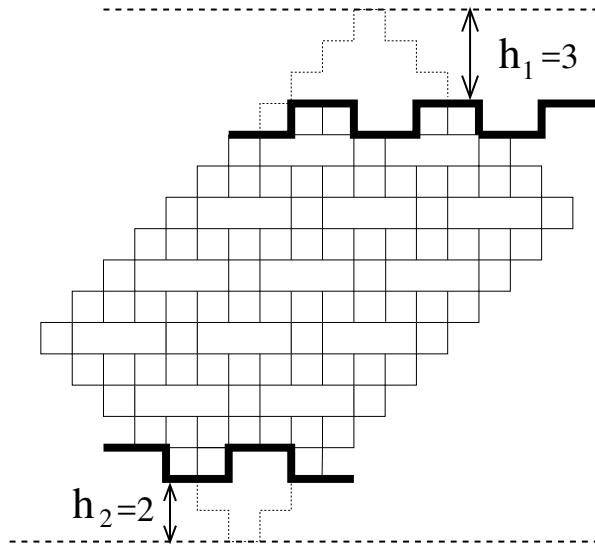


Figure 1.6: The graph  $TB_{4,7}^{3,6}$  is obtained by trimming the rectangle  $AR_{7,11}$  (on the lattice  $B$ ) by trimming two corners.

cut. Denote by  $TA_{m,n}^{h_1,h_2}$  the resulting trimmed Aztec rectangle. We notice that an edge of the zigzag cut is in the graph  $TA_{m,n}^{h_1,h_2}$  if and only if it is also a lattice edge in  $B$ . See Figure 1.5 for an example of the  $TA$ -graph; the dotted edges in the lower zigzag cut indicate the ones not in the  $TA$ -graph. We also have a variant of  $TA_{m,n}^{h_1,h_2}$  by applying the same process to the  $(2m-1) \times (2n-1)$  Aztec rectangle whose east-most edge is the *west-most* edge of a cross pattern on  $B$ . Denote by  $TB_{m,n}^{h_1,h_2}$  the resulting graph (see Figure 1.6). Ciucu [2] conjectured that

**Conjecture 1.2.** *The numbers of perfect matchings of  $TA_{m,n}^{h_1,h_2}$  and  $TB_{m,n}^{h_1,h_2}$  have only prime factors less than 13 in their prime factorizations.*

We prove Ciucu's conjecture by giving explicit formulas for the numbers of perfect matchings of  $TA_{m,n}^{h_1,h_2}$  and  $TB_{m,n}^{h_1,h_2}$  as follows. Given three integer numbers  $a, b, c$ , we define five functions  $g(a, b, c)$ ,  $q(a, b, c)$ ,  $\alpha(a, b, c)$ ,  $\beta(a, b, c)$ , and  $t(a, b)$  by setting

$$g(a, b, c) := (b-a)(b-c) + \left\lfloor \frac{(a-c)^2}{3} \right\rfloor, \quad (1.1)$$

$$q(a, b, c) := \left\lfloor \frac{(a-b+c)^2}{4} \right\rfloor, \quad (1.2)$$

$$\alpha(a, b, c) := \begin{cases} 2 & \text{if } 3b + a - c \equiv 1 \pmod{6}; \\ 3 & \text{if } 3b + a - c \equiv 5 \pmod{6}; \\ 1 & \text{otherwise,} \end{cases} \quad (1.3)$$

$$\beta(a, b, c) := \begin{cases} 3 & \text{if } 3b + a - c \equiv 1 \pmod{6}; \\ 2 & \text{if } 3b + a - c \equiv 5 \pmod{6}; \\ 1 & \text{otherwise,} \end{cases} \quad (1.4)$$

and

$$\tau(a, b) := \begin{cases} \frac{a+b}{2} & \text{if } h_1 \text{ and } h_2 \text{ are even;} \\ \frac{a}{2} & \text{if } h_1 \text{ is even and } h_2 \text{ is odd;} \\ \frac{b}{2} & \text{if } h_1 \text{ is odd and } h_2 \text{ is even;} \\ 0 & \text{otherwise.} \end{cases} \quad (1.5)$$

**Theorem 1.3.** Assume that  $\lfloor \frac{h_1+1}{2} \rfloor + \lfloor \frac{h_2+1}{2} \rfloor = 2(n-m)$ .

(a) The number of perfect matchings of the trimmed Aztec rectangle  $TA_{m,n}^{h_1, h_2}$  equals

$$\alpha(a, b, c) 2^{g(a, b, c+1)} 3^{\tau(h_1, h_2)} 5^{g(a, b, c)} 11^{q(a, b, c)}, \quad (1.6)$$

where  $a = m - \lfloor \frac{h_1+1}{2} \rfloor + 1$ ,  $b = n - \lfloor \frac{h_1+1}{2} \rfloor + 1$  and  $c = \lfloor \frac{h_2+1}{2} \rfloor$ .

(b) The number of perfect matchings of  $TB_{m,n}^{h_1, h_2}$  is

$$\beta(a', b', c') 2^{g(a', b', c'-1)} 3^{\tau(h_1+1, h_2+1)} 5^{g(a', b', c')} 11^{q(a', b', c')}, \quad (1.7)$$

where  $a' = m - \lfloor \frac{h_1+1}{2} \rfloor + 1$ ,  $b' = n - \lfloor \frac{h_1+1}{2} \rfloor + 1$  and  $c' = \lfloor \frac{h_2+1}{2} \rfloor$ .

It is easy to see that if a bipartite graph admits a perfect matching, then the numbers of vertices in its two vertex classes are the same. A bipartite graph satisfying the later balancing condition is called a *balanced graph*. If the condition  $\lfloor \frac{h_1+1}{2} \rfloor + \lfloor \frac{h_2+1}{2} \rfloor = 2(n-m)$  in Theorem 1.3 is violated, then both  $TA_{m,n}^{h_1, h_2}$  and  $TB_{m,n}^{h_1, h_2}$  are not balanced. Thus, their numbers of perfect matchings are 0.

The rest of this paper is organized as follows. In Section 2, we introduce six new families of subgraphs of the lattice  $B$  and present explicit formulas for the numbers of perfect matchings of these graphs (see Theorem 2.1). The theorem is the key result of our paper; and we will prove it in the next three sections. In Section 3, we prove several recurrences for the numbers of perfect matchings of the six families of graphs by using Kuo's graphical condensation method [9]. Then, in Section 4, we show that the formulas in Theorem 2.1 satisfy the same recurrences obtained in Section 3. This yields an inductive proof of Theorem 2.1, which is presented in Section 5. Section 6 is devoted to the proofs of Theorems 1.1 and 1.3 by using the result in Theorem 2.1. Finally, in Section 7, we investigate a hidden connection between the graph in Theorem 1.1 and the hexagonal dungeon introduced by Blum in his well-known conjecture (see [23], Problem 25). It is worth noticing that Blum's conjecture was confirmed by Ciucu and the author in [5].

## 2 Six new families of graphs

In this section, we consider six new families of graphs whose matching enumerations will be employed in our proofs of Theorems 1.1 and 1.3 in Section 6.

Pick the center  $V_s$  of a cross pattern on the lattice  $B$ . Let  $a, b, c, d, e, x$  be six non-negative integers. We create a six-sided contour starting from  $V_s$  as follows. We go  $2a\sqrt{2}$  units southeast from  $V_s$ , then  $2b\sqrt{2}$  units northeast,  $4c$  units west,  $2d\sqrt{2}$  units northwest, and  $2e\sqrt{2}$  units southwest. We adjust  $e$  so that the ending point  $V_e$  of the fifth side are

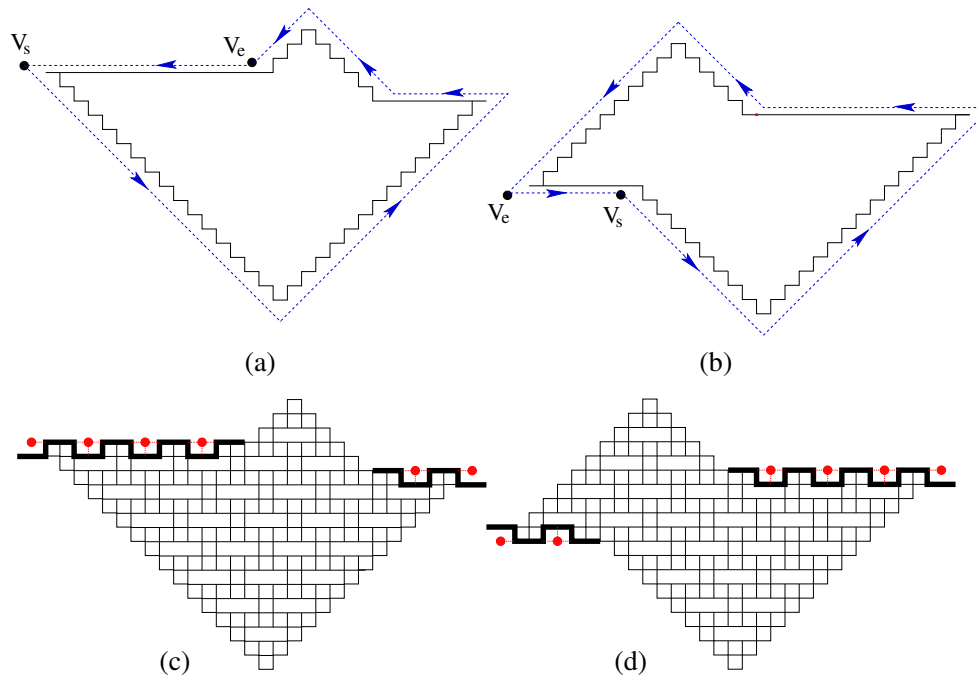


Figure 2.1: (a) The contour  $\mathcal{C}_{9,8,2}^{(1)}$  and the graph  $G_{9,8,2}$ . (b) The contour  $\mathcal{C}_{5,8,4}^{(1)}$  and the graph  $G_{5,8,4}$ . (c) Obtaining the graph  $F_{9,8,2}^{(1)}$  from the graph  $G_{9,8,2}$ . (d) Obtaining the graph  $F_{5,8,4}^{(1)}$  from  $G_{5,8,4}$ .

on the same level as  $V_s$ . Finally, we close the contour by going  $x$  units west or east, based on whether  $V_e$  is on the east or the west of  $V_s$  (see Figures 2.1(a) and (b)). We denote by  $\mathcal{C}^{(1)}(a, b, c)$  the resulting contour. We will show in the next three paragraphs that our contour depends on only three parameter  $a, b, c$ .

The above choice of  $e$  requires that

$$a + e = b + d.$$

If  $V_e$  is  $x$  units on the east of  $V_s$  (i.e.  $a > c + d$ ), then the closure of the contour yields  $4a = x + 4d + 4c$ , so  $x = 4(a - c - d)$ . Similarly, in the case when  $V_e$  is  $x$  units on the west of  $V_s$  (i.e.  $a < c + d$ ), we get  $x = 4(c + d - a)$ . Thus, in all cases, we must have  $x = 4f$ , where  $f = |a - c - d|$ .

We now consider the subgraph  $G_{a,b,c}$  of the lattice  $B$  induced by the vertices inside the contour (see the graphs restricted by the solid boundaries in Figures 2.1(a) and (b)). Next, along each horizontal side of the contour, we apply a zigzag cut as in the definition of the trimmed Aztec rectangles in the previous section (illustrated by bold zigzag lines in Figures 2.1(c) and (d); the shaded vertices indicate the vertices of  $G_{a,b,c}$ , which have been removed by the trimming process). In particular, for the  $c$ -side<sup>2</sup>, we perform the zigzag

<sup>2</sup>From now on, we usually call the first, the second, ..., the sixth sides of the contour the  $a$ -, the  $b$ -, ..., and the  $f$ -sides. The same terminology will be used for the sides of the graph induced by vertices inside the contour.

cut from right to left and stop when having no room on this side for the next step of the cut. Similarly, we cut along  $f$ -side from *left to right* and also stop when cannot reach further. Denote by  $F_{a,b,c}^{(1)}$  the resulting graph. (see Figure 2.1(c) for the case  $a > c + d$ , and Figure 2.1(d) for the case  $a \leq c + d$ ).

Recall that if a bipartite graph  $G$  admits a perfect matching, then the numbers of vertices in the two vertex classes of  $G$  must be the same; and we say that the graph  $G$  is *balanced*. One readily sees that the balance of  $F_{a,b,c}^{(1)}$  requires  $d = 2b - a - 2c$ . Moreover, to guarantee that the graph is not empty, we assume in addition  $b \geq 2$ . In summary, we have

$$d = 2b - a - 2c \geq 0, \tag{2.1}$$

$$e = b + d - a = 3b - 2a - 2c \geq 0, \tag{2.2}$$

and

$$f = |a - c - d| = |2a - 2b + c|. \tag{2.3}$$

It means that  $d, e, f$  depend on  $a, b, c$ . This explains why our graph  $F_{a,b,c}^{(1)}$  is indeed determined by  $a, b, c$  (and so is the contour  $\mathcal{C}^{(1)}(a, b, c)$ ).

Next, we consider a variant  $A_{a,b,c}^{(1)}$  of the graph  $F_{a,b,c}^{(1)}$  as follows. We remove all vertices along the  $a$ -,  $b$ -,  $d$ -, and  $e$ -sides of  $G_{a,b,c}$  (illustrated by white circles in Figures 2.2(a) and (b)). We now trim along the  $c$ - and  $f$ -sides of the resulting graph in the same way as in the definition of  $F_{a,b,c}^{(1)}$  (the vertices of  $G_{a,b,c}$ , which are removed by the trimming process, are illustrated by shaded points in Figures 2.2(a) and (b); the edges removed are shown by dotted edges). Figures 2.2(c) and (d) give examples of the graph  $A_{a,b,c}^{(1)}$  in the cases  $a > c + d$  and  $a \leq c + d$ , respectively.

In the definitions of the next families of graphs, we always assume the constraints (2.1), (2.2), (2.3), and  $b \geq 2$ .

In the spirit of the contour  $\mathcal{C}^{(1)}(a, b, c)$ , we define a new contour  $\mathcal{C}^{(2)}(a, b, c)$  as follows. Starting also from the center  $V_s$  of a cross pattern on the lattice  $B$ , we go  $2a\sqrt{2}$  units southwest, then  $4b$  units east,  $2c\sqrt{2}$  units northwest,  $2d\sqrt{2}$  units northeast,  $4e$  units west, and  $2f\sqrt{2}$  units northwest or southeast, depending on whether  $a > c + d$  or  $a \leq c + d$  (see Figures 2.3(a) and (b) for examples). The contour  $\mathcal{C}^{(2)}(a, b, c)$  determines a new induced subgraph  $H_{a,b,c}$  of the lattice  $B$  (i.e.,  $H_{a,b,c}$  is induced by vertices inside the contour). The graphs  $H_{9,8,2}$  and  $H_{5,8,4}$  are illustrated by the ones restricted by the solid boundaries in Figures 2.3(a) and (b), respectively.

Next, we remove all vertices along the  $a$ - and  $d$ -sides of  $H_{a,b,c}$ ; and we also remove the vertices along the  $f$ -side if  $a > c + d$  (see white circles in Figures 2.3(c) and (d)). Similar to the graph  $F_{a,b,c}^{(1)}$ , we obtain the graph  $F_{a,b,c}^{(2)}$  by applying the zigzag cuts along two horizontal sides of the resulting graph (which are now the  $b$ - and  $e$ -sides). The graphs  $F_{9,8,2}^{(2)}$  and  $F_{5,8,4}^{(2)}$  are pictured in Figures 2.3(c) and (d), respectively; the shaded points also indicate the vertices of  $H_{a,b,c}$ , which are removed by the trimming process.

Similarly, the graph  $A_{a,b,c}^{(2)}$  is obtained from  $H_{a,b,c}$  by removing vertices along the  $c$ -side, as well as vertices along the  $f$ -side when  $a \leq c + d$ , and trimming along two horizontal sides (illustrated in Figures 2.3(e) and (f)).

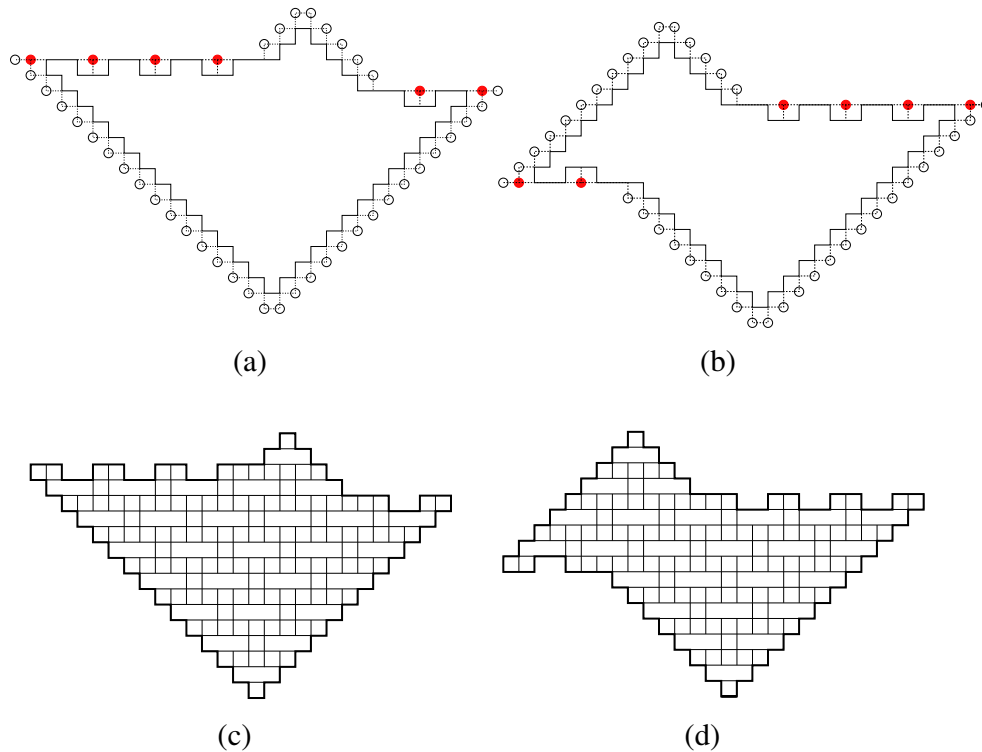


Figure 2.2: (a) Obtaining  $A_{9,8,2}^{(1)}$  from  $G_{9,8,2}$ . (b) Obtaining  $A_{5,8,4}^{(1)}$  from  $G_{5,8,4}$ . (c) The graph  $A_{9,8,2}^{(1)}$  with full details. (d) The graph  $A_{5,8,4}^{(1)}$  with full details.

We define next the third contour  $\mathcal{C}^{(3)}(a, b, c)$  in the same fashion as the previous ones. Starting the contour at the same point  $V_s$ , this time we go east, northwest, southwest, west, southeast, and finally southwest or northeast depending on whether  $a > c + d$  or  $a \leq c + d$ . The side-lengths of the contour are now  $4a$ ,  $2b\sqrt{2}$ ,  $2c\sqrt{2}$ ,  $4d$ ,  $2e\sqrt{2}$ , and  $2f\sqrt{2}$ , respectively (see Figures 2.4(a) and (b)). We denote by  $K_{a,b,c}$  the subgraph of the lattice  $B$  induced by the vertices inside  $\mathcal{C}_{a,b,c}^{(3)}$  (see the graph restricted by the solid contours in Figures 2.4(a) and (b)). Our last two graphs are obtained from  $K_{a,b,c}$  by a similar removing-trimming process as follows. The graph  $F_{a,b,c}^{(3)}$  is obtained from  $K_{a,b,c}$  by removing vertices along its  $b$ -,  $c$ -, and  $e$ -sides, as well as vertices along the  $f$ -side when  $a \leq c + d$ , and trimming along two horizontal sides (along the  $a$ -side from right to left, and the  $d$ -side from left to right). The graph  $A_{a,b,c}^{(3)}$  is obtained similarly by removing vertices along the  $f$ -side if  $a > c + d$ , and trimming along the two horizontal sides. Figures 2.4(c), (d), (e), and (f) show the graphs  $F_{9,8,2}^{(3)}$ ,  $F_{5,8,4}^{(3)}$ ,  $A_{9,8,2}^{(3)}$ , and  $A_{5,8,4}^{(3)}$ , respectively.

We show in the following theorem that, while  $A_{a,b,c}^{(i)}$ 's and  $F_{a,b,c}^{(i)}$ 's are non-symmetric and concave, their matching numbers are still given by perfect powers of small prime numbers.

**Theorem 2.1.** *Assume that  $a$ ,  $b$  and  $c$  are three non-negative integers satisfying  $b \geq 2$ ,*

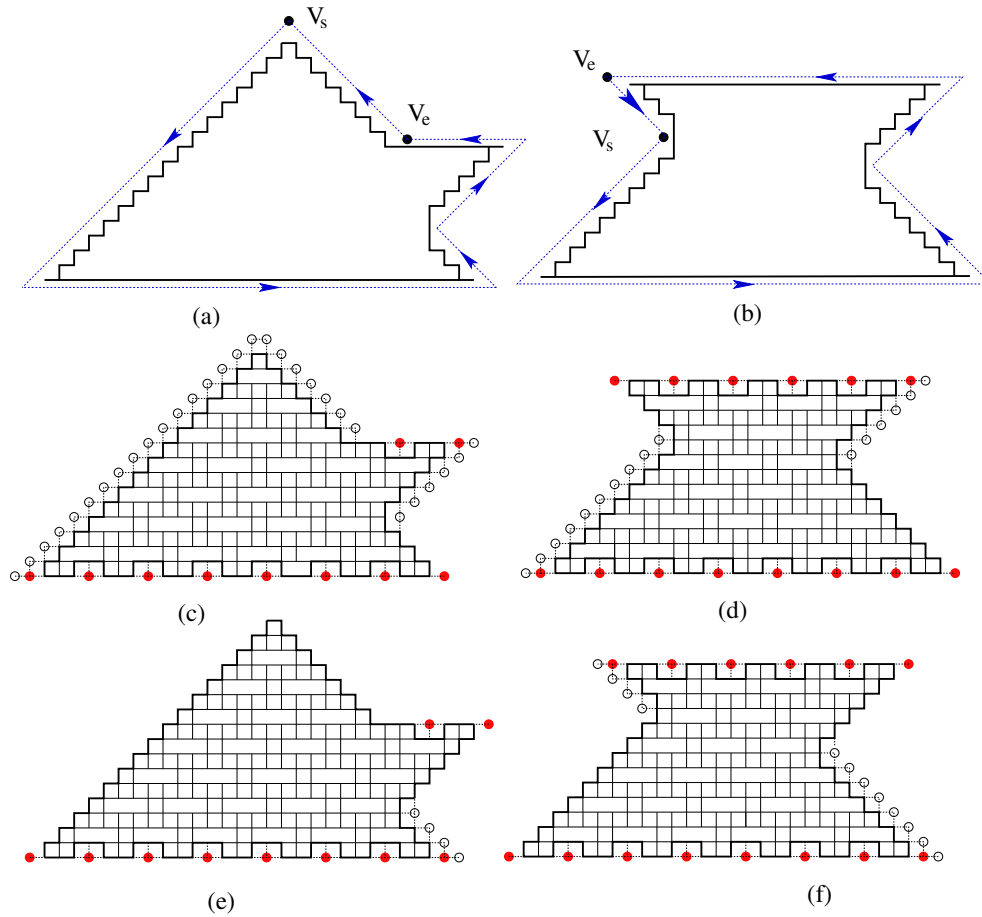


Figure 2.3: (a) The contour  $\mathcal{C}_{9,8,2}^{(2)}$  and the graph  $H_{9,8,2}$ . (b) The contour  $\mathcal{C}_{5,8,4}^{(2)}$  and the graph  $H_{5,8,4}$ . (c) The graph  $F_{9,8,2}^{(2)}$ . (d) The graph  $F_{5,8,4}^{(2)}$ . (e) The graph  $A_{9,8,2}^{(2)}$ . (f) The graph  $A_{5,8,4}^{(2)}$ .

$d := 2b - a - 2c \geq 0$ , and  $e := 3b - 2a - 2c \geq 0$ . Then

$$M\left(A_{a,b,c}^{(1)}\right) = \alpha(a, b, c)2^{g(a,b,c+1)}5^{g(a,b,c)}11^{q(a,b,c)}, \quad (2.4)$$

$$M\left(A_{a,b,c}^{(2)}\right) = \alpha(a, b, c)2^{g(a,b,c-1)-\lfloor(a-c+1)/3\rfloor+(a-b)}5^{g(a,b,c)}11^{q(a,b,c)}, \quad (2.5)$$

$$M\left(A_{a,b,c}^{(3)}\right) = \alpha(a, b, c)2^{g(a,b,c-1)-\lfloor(a-c+1)/3\rfloor}5^{g(a,b,c)}11^{q(a,b,c)}, \quad (2.6)$$

$$M\left(F_{a,b,c}^{(1)}\right) = \beta(a, b, c)2^{g(a,b,c-1)}5^{g(a,b,c)}11^{q(a,b,c)}, \quad (2.7)$$

$$M\left(F_{a,b,c}^{(2)}\right) = \beta(a, b, c)2^{g(a,b,c+1)+\lfloor(a-c+1)/3\rfloor-(a-b)}5^{g(a,b,c)}11^{q(a,b,c)}, \quad (2.8)$$

and

$$M\left(F_{a,b,c}^{(3)}\right) = \beta(a, b, c)2^{g(a,b,c+1)+\lfloor(a-c+1)/3\rfloor}5^{g(a,b,c)}11^{q(a,b,c)}, \quad (2.9)$$

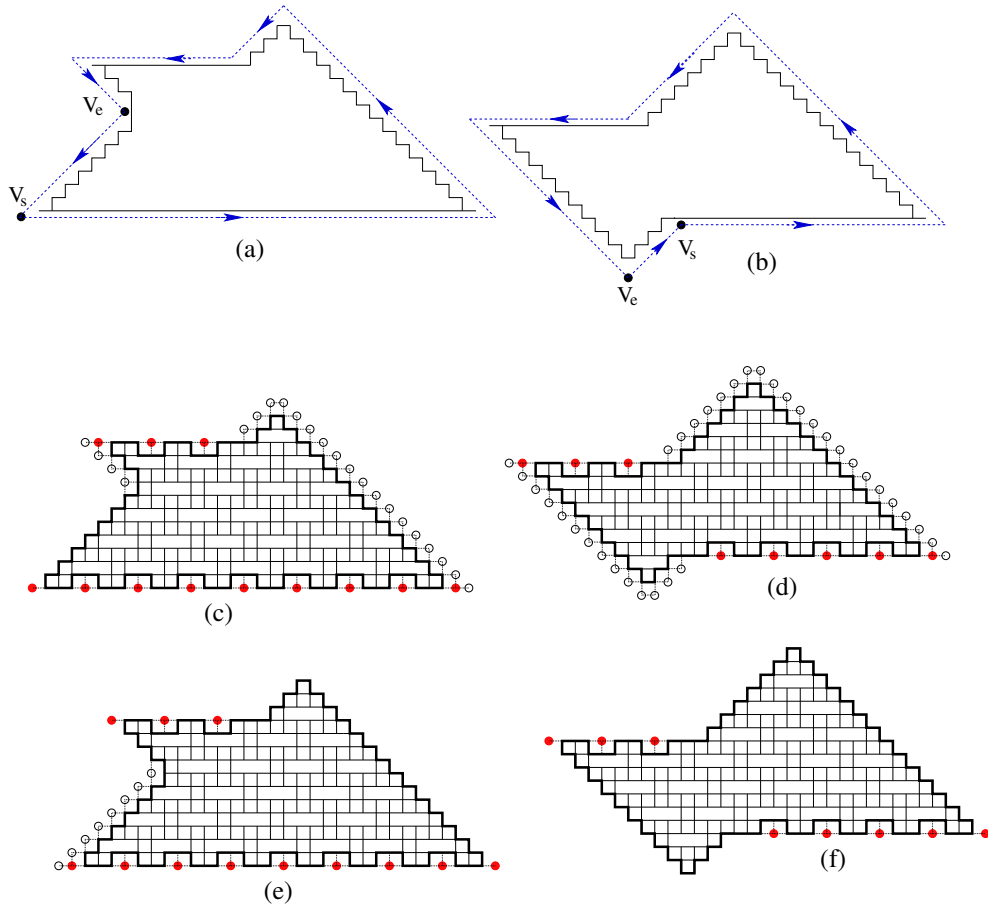


Figure 2.4: (a) The contour  $\mathcal{C}_{9,8,2}^{(3)}$  and the graph  $K_{9,8,2}$ . (b) The contour  $\mathcal{C}_{5,8,4}^{(3)}$  and the graph  $K_{5,8,4}$ . (c) The graph  $F_{9,8,2}^{(3)}$ . (d) The graph  $F_{5,8,4}^{(3)}$ . (e) The graph  $A_{9,8,2}^{(3)}$ . (f) The graph  $A_{5,8,4}^{(3)}$ .

where  $\alpha(a, b, c)$ ,  $\beta(a, b, c)$ ,  $q(a, b, c)$  and  $g(a, b, c)$  are defined as in Theorem 1.3, and where  $M(G)$  denotes the number of perfect matchings of a graph  $G$ .

The proof of Theorem 2.1 will be given in the next three sections. In particular, Sections 3 and 4 show that the expressions on the left and right hand sides of each of the equalities (2.4)–(2.9) both satisfy the same recurrences. Then we will give an inductive proof for the theorem in Section 5.

### 3 Recurrences of $M\left(A_{a,b,c}^{(i)}\right)$ and $M\left(F_{a,b,c}^{(i)}\right)$

Eric Kuo (re)proved the Aztec diamond theorem by Elkies, Kuperberg, Larsen, and Propp (see [6, 7]) by using a method called “graphical condensation” [9]. The key of his proof is the following combinatorial interpretation of the *Desnanot-Jacobi identity* in linear algebra (also mentioned as *Dodgson condensation*; see e.g. [11], pp. 136–149). We refer

the reader to [3, 4, 5, 14, 15, 16, 17, 18, 19, 20, 21, 22, 24, 25, 27] for various recent applications of this powerful method.

**Theorem 3.1** (Kuo's Condensation Theorem [9]). *Let  $G$  be a planar bipartite graph, and  $V_1$  and  $V_2$  the two vertex classes with  $|V_1| = |V_2|$ . Assume in addition that  $x, y, z$  and  $t$  are four vertices appearing in a cyclic order on a face of  $G$  so that  $x, z \in V_1$  and  $y, t \in V_2$ . Then*

$$M(G)M(G - \{x, y, z, t\}) = M(G - \{x, y\})M(G - \{z, t\}) + M(G - \{t, x\})M(G - \{y, z\}). \quad (3.1)$$

In this section, we use the Kuo's Condensation Theorem to prove that the numbers of perfect matchings of the six families of graphs  $A_{a,b,c}^{(i)}$ 's and  $F_{a,b,c}^{(i)}$ 's, for  $i = 1, 2, 3$ , satisfy the following six recurrences (with some constraints).

We use the notations  $\star(a, b, c)$  and  $\blacklozenge(a, b, c)$  for general functions from  $\mathbb{Z}^3$  to  $\mathbb{Z}$ . We consider the following six recurrences:

$$\begin{aligned} \star(a, b, c)\star(a - 3, b - 3, c - 2) &= \star(a - 2, b - 1, c)\star(a - 1, b - 2, c - 2) \\ &+ \star(a - 1, b - 1, c - 1)\star(a - 2, b - 2, c - 1), \end{aligned} \quad (R1)$$

$$\begin{aligned} \star(a, b, c)\star(a - 2, b - 2, c) &= \star(a - 1, b - 1, c)^2 \\ &+ \star(a, b, c + 1)\star(a - 2, b - 2, c - 1), \end{aligned} \quad (R2)$$

$$\begin{aligned} \star(a, b, 0)\star(a - 2, b - 2, 0) &= \star(a - 1, b - 1, 0)^2 \\ &+ \star(a, b, 1)\star(3b - 2a, 2b - a, 1), \end{aligned} \quad (R3)$$

$$\begin{aligned} \star(a, b, c)\star(a - 2, b - 3, c - 2) &= \star(a - 1, b - 1, c)\star(a - 1, b - 2, c - 2) \\ &+ \star(a - 2, b - 2, c - 1)\star(a, b - 1, c - 1), \end{aligned} \quad (R4)$$

$$\left\{ \begin{aligned} \star(a, b, c)\star(a - 2, b - 3, c - 2) &= \blacklozenge(c, b - 1, a - 1)\star(a - 1, b - 2, c - 2) \\ &+ \star(a - 2, b - 2, c - 1)\star(a, b - 1, c - 1); \\ \blacklozenge(a, b, c)\blacklozenge(a - 2, b - 3, c - 2) &= \star(c, b - 1, a - 1)\blacklozenge(a - 1, b - 2, c - 2) \\ &+ \blacklozenge(a - 2, b - 2, c - 1)\blacklozenge(a, b - 1, c - 1), \end{aligned} \right. \quad (R5)$$

and

$$\left\{ \begin{aligned} \star(a, b, 0)\star(a - 2, b - 2, 0) &= \star(a - 1, b - 1, 0)^2 \\ &+ \star(a, b, 1)\blacklozenge(3b - 2a, 2b - a, 1); \\ \blacklozenge(a, b, 0)\blacklozenge(a - 2, b - 2, 0) &= \blacklozenge(a - 1, b - 1, 0)^2 \\ &+ \blacklozenge(a, b, 1)\star(3b - 2a, 2b - a, 1). \end{aligned} \right. \quad (R6)$$

We notice that if  $\star \equiv \blacklozenge$  in the recurrence (R6), we get the recurrence (R3).

**Lemma 3.2.** Let  $a, b$  and  $c$  be non-negative integers so that  $b \geq 5, c \geq 2, d := 2b - a - 2c \geq 0, e := 3b - 2a - 2c \geq 0$ , and  $a > c + d$ . Then for  $i = 1, 2, 3$  the numbers of perfect matchings  $M(A_{a,b,c}^{(i)})$  and  $M(F_{a,b,c}^{(i)})$  all satisfy the recurrence (R1), i.e. we have

$$M\left(A_{a,b,c}^{(i)}\right) M\left(A_{a-3,b-3,c-2}^{(i)}\right) = M\left(A_{a-2,b-1,c}^{(i)}\right) M\left(A_{a-1,b-2,c-2}^{(i)}\right) + M\left(A_{a-1,b-1,c-1}^{(i)}\right) M\left(A_{a-2,b-2,c-1}^{(i)}\right) \quad (3.2)$$

and

$$M\left(F_{a,b,c}^{(i)}\right) M\left(F_{a-3,b-3,c-2}^{(i)}\right) = M\left(F_{a-2,b-1,c}^{(i)}\right) M\left(F_{a-1,b-2,c-2}^{(i)}\right) + M\left(F_{a-1,b-1,c-1}^{(i)}\right) M\left(F_{a-2,b-2,c-1}^{(i)}\right). \quad (3.3)$$

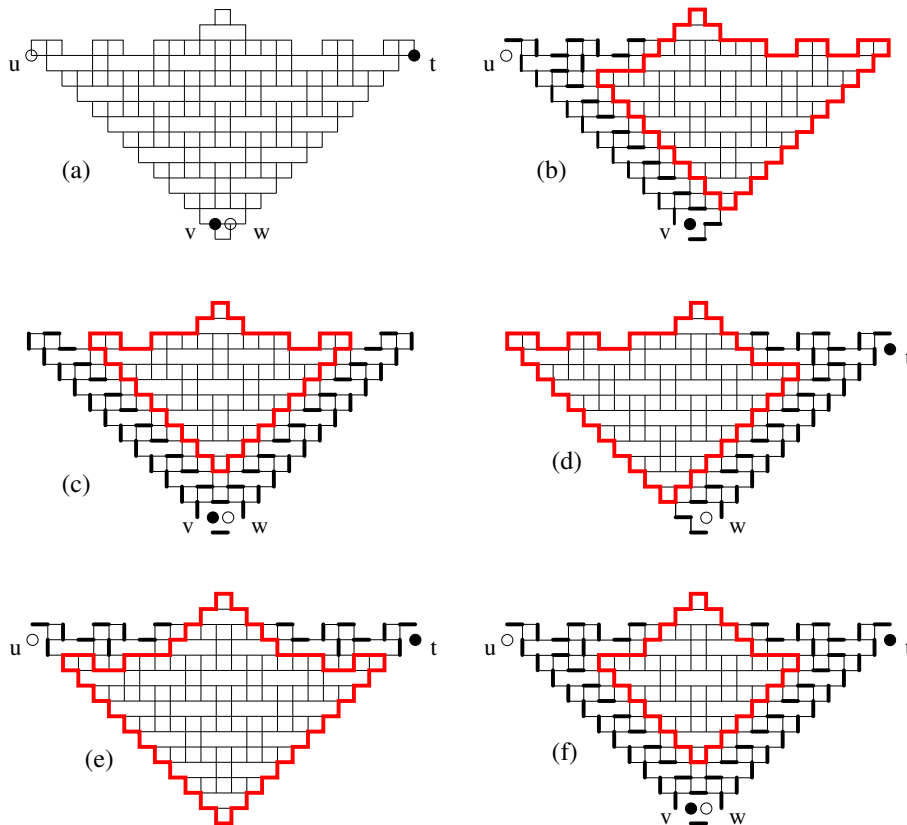


Figure 3.1: Illustrating the proof of Lemma 3.2.

*Proof.* First, we prove the equality (3.2), for  $i = 1$ .

Apply Kuo's Condensation Theorem 3.1 to the graphs  $G := A_{a,b,c}^{(1)}$  with the four vertices  $u, v, w, t$  chosen as in Figure 3.1(a) (for  $a = b = 8$  and  $c = 3$ ). In particular, we pick  $u$  on the west corner,  $v$  and  $w$  on the south corner, and  $t$  on the east corner of the graph.

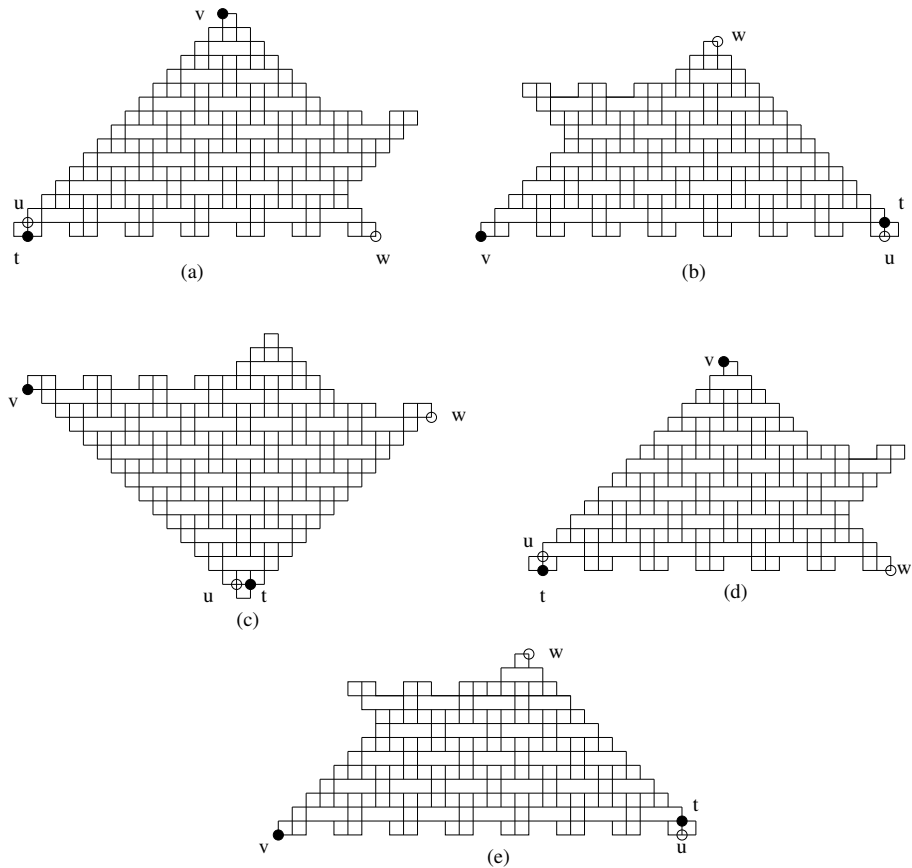


Figure 3.2: Illustrating the proof of Lemma 3.2.

Consider the graph  $G - \{u, v\}$ . There are several edges that are forced to be in any perfect matchings of the graph (see the graph restricted by the bold contour in Figure 3.1(b)). The removal of these forced edges does not change the number of perfect matchings of  $G - \{u, v\}$ . By removing the forced edges we obtain a graph isomorphic to  $A_{a-2, b-1, c}^{(1)}$  (see the graph restricted by the bold contour in Figure 3.1(b)), and get

$$M(G - \{u, v\}) = M(A_{a-2, b-1, c}^{(1)}).$$

Similarly, we have

$$M(G - \{v, w\}) = M(A_{a-1, b-2, c-2}^{(1)}) \text{ (see Figure 3.1(c))},$$

$$M(G - \{w, t\}) = M(A_{a-1, b-1, c-1}^{(1)}) \text{ (see Figure 3.1(d))},$$

$$M(G - \{t, u\}) = M(A_{a-2, b-2, c-1}^{(1)}) \text{ (see Figure 3.1(e))},$$

and

$$M(G - \{u, v, w, t\}) = M(A_{a-3, b-3, c-2}^{(1)}) \text{ (see Figure 3.1(f))}.$$

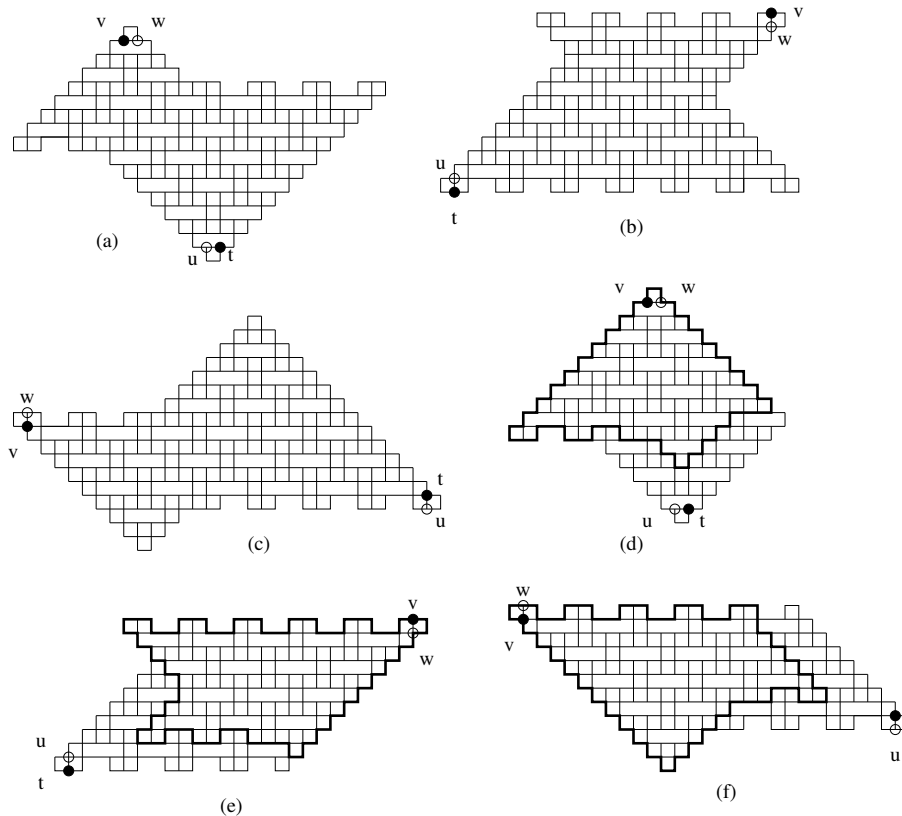


Figure 3.3: the graphs  $A_{5,8,4}^{(1)}$  (a),  $A_{5,8,4}^{(2)}$  (b),  $A_{5,8,4}^{(3)}$  (c),  $A_{4,5,0}^{(1)}$  (d),  $A_{4,5,0}^{(2)}$  (e), and  $A_{4,5,0}^{(3)}$  (f) with the four vertices  $u, v, w, t$  in Lemma 3.3.

Substituting the above five equalities into the equality (3.1) in Kuo's Condensation Theorem, we get (3.2), for  $i = 1$ .

Similarly, apply Kuo's Condensation Theorem 3.1 to the graphs  $A_{a,b,c}^{(2)}$  and  $A_{a,b,c}^{(3)}$  with the four vertices  $u, v, w, t$  chosen as in Figures 3.2(a) and (b), respectively, we get the equality (3.2), for  $i = 2, 3$ .

Finally, (3.3) is obtained by repeating the above arguments to the graphs  $F_{a,b,c}^{(i)}$ 's with the four vertices  $u, v, w, t$  selected as in Figures 3.2(c), (d), and (e).  $\square$

**Lemma 3.3.** *Let  $a, b$  and  $c$  be non-negative integers satisfying  $a \geq 2$ ,  $b \geq 4$ ,  $d := 2b - a - 2c \geq 2$ , and  $e := 3b - 2a - 2c \geq 2$ .*

(a) *If  $c \geq 1$ , then  $M(A_{a,b,c}^{(i)})$  and  $M(F_{a,b,c}^{(i)})$  all satisfy the recurrence (R2), for  $i = 1, 2, 3$ .*

(b) *If  $c = 0$ , then  $M(A_{a,b,0}^{(1)})$  and  $M(F_{a,b,0}^{(1)})$  both satisfy the recurrence (R3). Moreover, for  $i = 2, 3$  the two pairs of numbers of perfect matchings  $(M(A_{a,b,0}^{(i)}), M(A_{a,b,0}^{(5-i)}))$  and  $(M(F_{a,b,0}^{(i)}), M(F_{a,b,0}^{(5-i)}))$  both satisfy the recurrence (R6) for  $(\star, \blacklozenge)$ .*

*Proof.* (a) We prove only the statement for the  $A$ -graphs, as the statement for  $F$ -graphs

can be obtained similarly. We need to show for  $i = 1, 2, 3$  that

$$M\left(A_{a,b,c}^{(i)}\right) M\left(A_{a-2,b-2,c}^{(i)}\right) = M\left(A_{a-1,b-1,c}^{(i)}\right)^2 + M\left(A_{a,b,c+1}^{(i)}\right) M\left(A_{a-2,b-2,c-1}^{(i)}\right). \quad (3.4)$$

Consider the graphs  $A_{a,b,c}^{(i)}$  with the four vertices  $u, v, w, t$  located as in Figures 3.3(a), (b), and (c), for  $i = 1, 2, 3$  respectively. Similar to the proof of Lemma 3.2, we have

$$M(G - \{u, v\}) = M(A_{a-1,b-1,c}^{(i)}), \quad (3.5)$$

$$M(G - \{v, w\}) = M(A_{a-1,b-1,c}^{(i)}), \quad (3.6)$$

$$M(G - \{w, t\}) = M(A_{a,b,c+1}^{(i)}), \quad (3.7)$$

$$M(G - \{t, u\}) = M(A_{a-2,b-2,c-1}^{(i)}), \quad (3.8)$$

$$M(G - \{u, v, w, t\}) = M(A_{a-2,b-2,c}^{(i)}). \quad (3.9)$$

Again, by Kuo's Theorem, we get (3.4).

(b) We prove the statement for the graphs  $A_{a,b,c}^{(i)}$ 's, and the one for  $F_{a,b,c}^{(i)}$ 's can be obtained in an analogous manner. In particular, we need to show that

$$M\left(A_{a,b,0}^{(1)}\right) M\left(A_{a-2,b-2,0}^{(1)}\right) = M\left(A_{a-1,b-1,0}^{(1)}\right)^2 + M\left(A_{a,b,1}^{(1)}\right) M\left(A_{e,d,1}^{(1)}\right), \quad (3.10)$$

and that for  $i = 2, 3$

$$M\left(A_{a,b,0}^{(i)}\right) M\left(A_{a-2,b-2,0}^{(i)}\right) = M\left(A_{a-1,b-1,0}^{(i)}\right)^2 + M\left(A_{a,b,1}^{(i)}\right) M\left(A_{e,d,1}^{(5-i)}\right). \quad (3.11)$$

The equalities (3.10) and (3.11) can be treated similarly to (3.4). We still pick the four vertices  $u, v, w, t$  in the graphs  $A_{a,b,0}^{(i)}$ 's as in Figures 3.3(d), (e), and (f). We also get the equalities (3.5), (3.6), (3.7), and (3.9), for  $c = 0$ . However, the graph obtained by removing forced edges from the graph  $A_{a,b,c}^{(i)} - \{u, t\}$  is not  $A_{a-2,b-2,c-1}^{(i)}$  any more (the latter graph is *not* defined when  $c = 0$ ); and it is now isomorphic to  $A_{e,d,1}^{(1)}$  (resp.,  $A_{e,d,1}^{(3)}$ ,  $A_{e,d,1}^{(2)}$ ), where  $d = 2b - a$  and  $e = 3b - 2a$ . The graphs  $A_{e,d,1}^{(1)}$ ,  $A_{e,d,1}^{(3)}$ ,  $A_{e,d,1}^{(2)}$  are illustrated by the ones restricted by the bold contours in Figures 3.3(d), (e), and (f), respectively. Thus, we have

$$M(A_{a,b,0}^{(1)} - \{t, u\}) = M(A_{e,d,1}^{(1)}), \quad (3.12)$$

$$M(A_{a,b,0}^{(2)} - \{t, u\}) = M(A_{e,d,1}^{(3)}), \quad (3.13)$$

and

$$M(A_{a,b,0}^{(3)} - \{t, u\}) = M(A_{e,d,1}^{(2)}). \quad (3.14)$$

Then (3.10) and (3.11) follow from Theorem 3.1.  $\square$

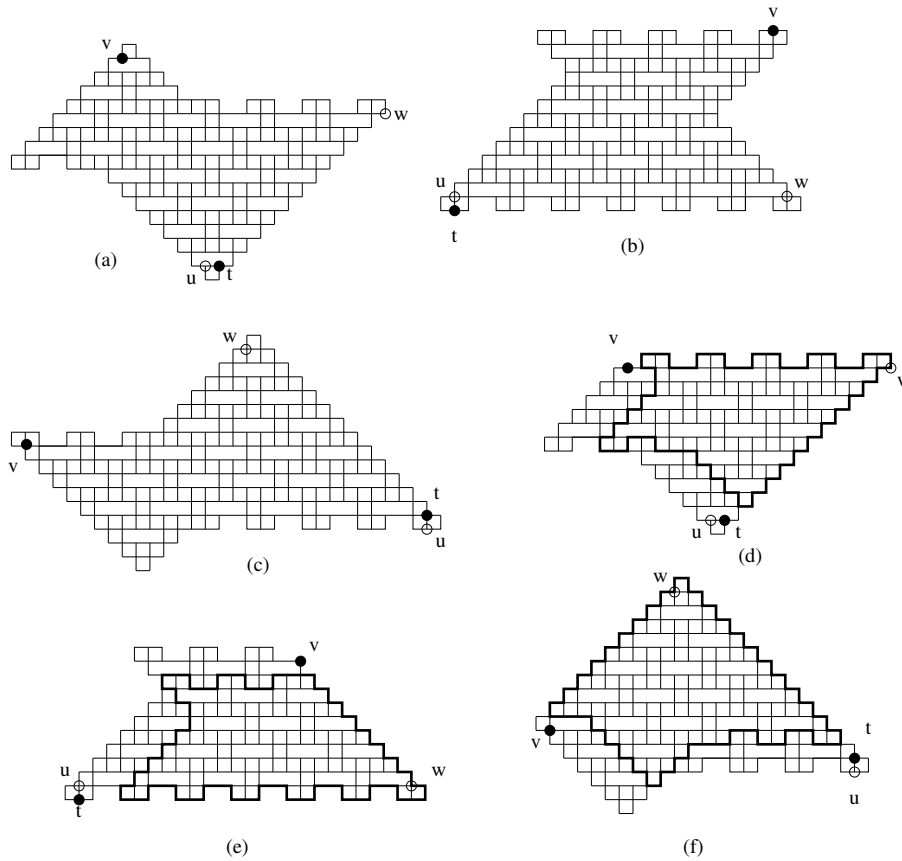


Figure 3.4: The graphs  $A_{5,8,4}^{(1)}$  (a),  $A_{5,8,4}^{(2)}$  (b),  $A_{5,8,4}^{(3)}$  (c),  $A_{4,8,6}^{(1)}$  (d),  $A_{4,8,6}^{(2)}$  (e), and  $A_{4,8,6}^{(3)}$  (f) with the selection of the vertices  $u, v, w, t$  in Lemma 3.4.

**Lemma 3.4.** *Assume that  $a, b, c$  are three non-negative integers satisfying  $a \geq 2$ ,  $b \geq 5$ ,  $c \geq 2$ ,  $d := 2b - a - 2c \geq 0$ , and  $e := 3b - 2a - 2c \geq 0$ . Assume in addition that  $a \leq c + d$ .*

(a) *If  $d \geq 1$ , then for  $i = 1, 2, 3$  the numbers perfect matchings  $M(A_{a,b,c}^{(i)})$  and  $M(F_{a,b,c}^{(i)})$  all satisfy the recurrence (R4).*

(b) *If  $d = 0$ , then for  $i = 1, 2, 3$  the pairs of the numbers of perfect matchings  $(M(A_{a,b,c}^{(i)}), M(F_{a,b,c}^{(4-i)}))$  and  $(M(A_{a,b,c}^{(i)}), M(F_{a,b,c}^{(4-i)}))$  both satisfy the recurrence (R5) for  $(\star, \blacklozenge)$ .*

*Proof.* (a) We prove here the number of perfect matchings of  $A_{a,b,c}^{(i)}$ 's satisfies the recurrence (R4), and the corresponding statement for  $F_{a,b,c}^{(i)}$ 's can be obtained in the same fashion.

We need to show that

$$\begin{aligned}
 M\left(A_{a,b,c}^{(i)}\right) M\left(A_{a-2,b-3,c-2}^{(i)}\right) &= M\left(A_{a-1,b-1,c}^{(i)}\right) M\left(A_{a-1,b-2,c-2}^{(i)}\right) \\
 &\quad + M\left(A_{a-2,b-2,c-1}^{(i)}\right) M\left(A_{a,b-1,c-1}^{(i)}\right),
 \end{aligned}
 \tag{3.15}$$

for  $i = 1, 2, 3$ .

Similar to Lemmas 3.2 and 3.3, we apply Kuo's Theorem 3.1 to the graph  $A_{a,b,c}^{(i)}$  with the four vertices  $u, v, w, t$  chosen as in Figures 3.4(a), (b), and (c). By considering forced edges, we have the following equalities:

$$M(G - \{u, v\}) = M(A_{a-1,b-1,c}^{(i)}), \quad (3.16)$$

$$M(G - \{v, w\}) = M(A_{a,b-1,c-1}^{(i)}), \quad (3.17)$$

$$M(G - \{w, t\}) = M(A_{a-1,b-2,c-2}^{(i)}), \quad (3.18)$$

$$M(G - \{t, u\}) = M(A_{a-2,b-2,c-1}^{(i)}), \quad (3.19)$$

$$M(G - \{u, v, w, t\}) = M(A_{a-2,b-3,c-2}^{(i)}). \quad (3.20)$$

We get (3.15) by substituting (3.16)–(3.20) into the equality (3.1) in Kuo's Theorem 3.1.

(b) First, we note that if  $d := 2b - a - 2c = 0$  as in the part (b) of Lemma 3.4, then  $2(b - 1) - (a - 1) - 2c = -1$ . It means that the graphs  $A_{a-1,b-1,c}^{(i)}$  and  $F_{a-1,b-1,c}^{(i)}$  do not exist in this case (otherwise the  $d$ -sides of the contour  $C^{(i)}(a - 1, b - 1, c)$  has a negative length, a contradiction).

The similarity between the statement for the  $A$ - and the statement for the  $B$ -graphs allows us to prove only first one. This part can be treated like part (a) by applying Kuo's Theorem 3.1 to the graphs  $A_{a,b,c}^{(i)}$ 's with the four vertices  $u, v, w, t$  selected as in Figures 3.4(d), (e), and (f). The only difference here is that, after removing forced edges from the graph  $A_{a,b,c}^{(i)} - \{u, v\}$ , we get the graph  $F_{c,b-1,a-1}^{(4-i)}$  (see the graphs restricted by the bold contours in Figures 3.4(d), (e), and (f)), instead of the graph  $A_{a-1,b-1,c}^{(i)}$  as in the part (a).  $\square$

For  $i = 1, 2, 3$  denote by  $\Phi_i(a, b, c)$  the product on the right hand sides of the equalities (2.4)–(2.6) in Theorem 2.1, respectively, and  $\Psi_i(a, b, c)$  the product on the right hand sides of equalities (2.7)–(2.9), respectively. In the next section, we will show that these functions satisfy the same recurrences (R1)–(R6).

## 4 Recurrences for the functions $\Phi_i(a, b, c)$ and $\Psi_i(a, b, c)$

**Lemma 4.1.** *For any integers  $a, b, c$ , and  $i = 1, 2, 3$ , the functions  $\Phi_i(a, b, c)$  and  $\Psi_i(a, b, c)$  all satisfy the recurrence (R1).*

*Proof.* We need to show that

$$\begin{aligned} \Phi_i(a, b, c)\Phi_i(a - 3, b - 3, c - 2) &= \Phi_i(a - 2, b - 1, c)\Phi_i(a - 1, b - 2, c - 2) \\ &\quad + \Phi_i(a - 1, b - 1, c - 1)\Phi_i(a - 2, b - 2, c - 1) \end{aligned} \quad (4.1)$$

and

$$\begin{aligned} \Psi_i(a, b, c)\Psi_i(a - 3, b - 3, c - 2) &= \Psi_i(a - 2, b - 1, c)\Psi_i(a - 1, b - 2, c - 2) \\ &+ \Psi_i(a - 1, b - 1, c - 1)\Psi_i(a - 2, b - 2, c - 1), \end{aligned} \quad (4.2)$$

for  $i = 1, 2, 3$ .

We first consider the case of even  $b$ . There are six subcases to distinguish, based on the values of  $a - c \pmod{6}$ . We show in details here the subcase when  $a - c \equiv 0 \pmod{6}$  (the other five subcases can be obtained in a perfectly analogous manner).

If  $a - c \equiv 0 \pmod{6}$ , by the definition of functions  $g(a, b, c)$  and  $q(a, b, c)$ , we can cancel out almost all the exponents of 2, 5 and 11 on both sides of the equalities (4.1) and (4.2). The equality (4.1) becomes

$$\begin{aligned} 11\alpha(a, b, c)\alpha(a - 3, b - 3, c - 2) &= 2\alpha(a - 2, b - 1, c)\alpha(a - 1, b - 2, c - 2) \\ &+ \alpha(a - 1, b - 1, c - 1)\alpha(a - 2, b - 2, c - 1); \end{aligned} \quad (4.3)$$

and the equality (4.2) becomes

$$\begin{aligned} 11\beta(a, b, c)\beta(a - 3, b - 3, c - 2) &= \beta(a - 2, b - 1, c)\beta(a - 1, b - 2, c - 2) \\ &+ \beta(a - 1, b - 1, c - 1)\beta(a - 2, b - 2, c - 1). \end{aligned} \quad (4.4)$$

By definition of the functions  $\alpha(a, b, c)$  and  $\beta(a, b, c)$ , we have here  $\alpha(a, b, c) = 1$ ,  $\alpha(a - 3, b - 3, c - 2) = 1$ ,  $\alpha(a - 2, b - 1, c) = 2$ ,  $\alpha(a - 1, b - 2, c - 2) = 2$ ,  $\alpha(a - 1, b - 1, c - 1) = 1$ ,  $\alpha(a - 2, b - 2, c - 1) = 3$ ,  $\beta(a, b, c) = 1$ ,  $\beta(a - 3, b - 3, c - 2) = 1$ ,  $\beta(a - 2, b - 1, c) = 2$ ,  $\beta(a - 1, b - 2, c - 2) = 3$ ,  $\beta(a - 1, b - 1, c - 1) = 1$ , and  $\beta(a - 2, b - 2, c - 1) = 2$ . Then the above equalities are equivalent to the following obvious equalities

$$11 \cdot 1 \cdot 1 = 2 \cdot 2 \cdot 2 + 1 \cdot 3$$

and

$$11 \cdot 1 \cdot 1 = 3 \cdot 3 + 1 \cdot 2,$$

respectively.

The remaining case of odd  $b$  turns out to follow from the case of even  $b$ . Indeed, for  $j = 0, 1, \dots, 5$ , verification of the case of odd  $b$  and  $a - c \equiv j \pmod{6}$  is the same as the verification of the case of even  $b$  and  $a - c \equiv 3 + j \pmod{6}$ .  $\square$

**Lemma 4.2.** (a) For any integers  $a, b, c$ , and  $i = 1, 2, 3$ , the functions  $\Phi_i(a, b, c)$  and  $\Psi_i(a, b, c)$  also satisfy the recurrence (R2), i.e.

$$\begin{aligned} \Phi_i(a, b, c)\Phi_i(a - 2, b - 2, c) &= \Phi_i^2(a - 1, b - 1, c) \\ &+ \Phi_i(a, b, c + 1)\Phi_i(a - 2, b - 2, c - 1) \end{aligned} \quad (4.5)$$

and

$$\begin{aligned} \Psi_i(a, b, c)\Psi_i(a - 2, b - 2, c) &= \Psi_i^2(a - 1, b - 1, c) \\ &+ \Psi_i(a, b, c + 1)\Psi_i(a - 2, b - 2, c - 1), \end{aligned} \quad (4.6)$$

for  $i = 1, 2, 3$ .

(b) The function  $\Phi_1(a, b, c)$  and  $\Psi_1(a, b, c)$  both satisfy the recurrence (R3), i.e.

$$\begin{aligned} \Phi_1(a, b, 0)\Phi_1(a - 2, b - 2, 0) &= \Phi_1^2(a - 1, b - 1, 0) \\ &+ \Phi_1(a, b, 1)\Phi_1(3b - 2a, 2b - a, 1) \end{aligned} \quad (4.7)$$

and

$$\begin{aligned} \Psi_1(a, b, 0)\Psi_1(a - 2, b - 2, 0) &= \Psi_1^2(a - 1, b - 1, 0) \\ &+ \Psi_1(a, b, 1)\Psi_1(3b - 2a, 2b - a, 1). \end{aligned} \quad (4.8)$$

Moreover, for  $i = 2, 3$ , the pairs of functions  $(\Phi_i(a, b, c), \Phi_{5-i}(a, b, c))$  and  $(\Psi_i(a, b, c), \Psi_{5-i}(a, b, c))$  both satisfy the recurrence (R6) for  $(\star, \diamond)$ , i.e.

$$\begin{aligned} \Phi_i(a, b, 0)\Phi_i(a - 2, b - 2, 0) &= \Phi_i^2(a - 1, b - 1, 0) \\ &+ \Phi_i(a, b, 1)\Phi_{5-i}(3b - 2a, 2b - a, 1) \end{aligned} \quad (4.9)$$

and

$$\begin{aligned} \Psi_i(a, b, 0)\Psi_i(a - 2, b - 2, 0) &= \Psi_i^2(a - 1, b - 1, 0) \\ &+ \Psi_i(a, b, 1)\Psi_{5-i}(3b - 2a, 2b - a, 1), \end{aligned} \quad (4.10)$$

for  $i = 2, 3$ .

*Proof.* (a) Arguing the same as the proof of Lemma 4.1, we only need to consider the case of even  $b$ .

When  $b$  is even, we have also six subcases to distinguish, depending on the values of  $a - c \pmod{6}$ . Again, we only show here the verification for the subcase  $a - c \equiv 0 \pmod{6}$ , and the other subcases can be obtained similarly.

Assume now that  $a - c$  is a multiple of 6. Similar to Lemma 4.1, we can cancel out almost all the exponents of 2, 5 and 11 on two sides of the equalities (4.5) and (4.6). These equalities are simplified to

$$\begin{aligned} 10\alpha(a, b, c)\alpha(a - 2, b - 2, c) &= \alpha^2(a - 1, b - 1, c) \\ &+ \alpha(a, b, c + 1)\alpha(a - 2, b - 2, c - 1) \end{aligned} \quad (4.11)$$

and

$$\begin{aligned} 5\beta(a, b, c)\beta(a - 2, b - 2, c) &= \beta^2(a - 1, b - 1, c) \\ &+ \beta(a, b, c + 1)\beta(a - 2, b - 2, c - 1), \end{aligned} \quad (4.12)$$

respectively. By the definition of  $\alpha(a, b, c)$  and  $\beta(a, b, c)$ , one can verify easily the above equalities.

(b) We only show that  $\Phi_1(a, b, c)$  and  $\Psi_1(a, b, c)$  satisfy (R3), as the second statement can be proven similarly.

By definition of functions  $\Phi_1$  and  $\Psi_1$ , one readily verifies that

$$\Phi_1(a-2, b-2, -1) = \Phi_1(3b-2a, 2b-a, 1) \quad (4.13)$$

and

$$\Psi_1(a-2, b-2, -1) = \Psi_1(3b-2a, 2b-a, 1), \quad (4.14)$$

then (4.7) and (4.8) follow from part (a), for  $c = 0$ .  $\square$

**Lemma 4.3.** *a) For any integers  $a, b, c$  and  $i = 1, 2, 3$ , the functions  $\Phi_i(a, b, c)$  and  $\Psi_i(a, b, c)$  satisfy the recurrence (R4), i.e.*

$$\begin{aligned} \Phi_i(a, b, c)\Phi_i(a-2, b-3, c-2) &= \Phi_i(a-1, b-1, c)\Phi_i(a-1, b-2, c-2) \\ &+ \Phi_i(a-2, b-2, c-1)\Phi_i(a, b-1, c-1) \end{aligned} \quad (4.15)$$

and

$$\begin{aligned} \Psi_i(a, b, c)\Psi_i(a-2, b-3, c-2) &= \Psi_i(a-1, b-1, c)\Psi_i(a-1, b-2, c-2) \\ &+ \Psi_i(a-2, b-2, c-1)\Psi_i(a, b-1, c-1), \end{aligned} \quad (4.16)$$

for  $i = 1, 2, 3$ .

*(b) For  $i = 1, 2, 3$ , the pairs of functions  $(\Phi_i(a, b, c), \Psi_{4-i}(a, b, c))$  and  $(\Psi_i(a, b, c), \Phi_{4-i}(a, b, c))$  all satisfy the recurrence (R5), i.e.*

$$\begin{aligned} \Phi_i(a, b, c)\Phi_i(a-2, b-3, c-2) &= \Psi_{4-i}(c, b-1, a-1)\Phi_i(a-1, b-2, c-2) \\ &+ \Phi_i(a-2, b-2, c-1)\Phi_i(a, b-1, c-1) \end{aligned} \quad (4.17)$$

and

$$\begin{aligned} \Psi_i(a, b, c)\Psi_i(a-2, b-3, c-2) &= \Phi_{4-i}(c, b-1, a-1)\Psi_i(a-1, b-2, c-2) \\ &+ \Psi_i(a-2, b-2, c-1)\Psi_i(a, b-1, c-1), \end{aligned} \quad (4.18)$$

for  $i = 1, 2, 3$ .

*Proof.* (a) This part can be treated similarly to Lemma 4.1 and Lemma 4.2(a).

(b) From part (a), we only need to prove that

$$\Psi_i(a-1, b-1, c) = \Phi_{4-i}(c, b-1, a-1) \quad (4.19)$$

and

$$\Phi_i(a-1, b-1, c) = \Psi_{4-i}(c, b-1, a-1), \quad (4.20)$$

for  $i = 1, 2, 3$ . However, this follows directly from the definition of the functions  $\Phi_i$ 's and  $\Psi_i$ 's.  $\square$

## 5 Proof of Theorem 2.1

We will prove Theorem 2.1 in the same fashion as the proof of Theorem 3.1 in [5].

*Proof of Theorem 2.1.* We define the a function  $P(a, b, c)$  by setting

$$P(a, b, c) := a + b + c + d + e + f,$$

where  $d := 2b - a - 2c$ ,  $e := 3b - 2a - 2c$ , and  $f := |2a - 2b + c|$  as usual. Moreover, one readily sees that  $P(a, b, c)$  equals  $4b - 2c$  if  $a > c + d$ , and  $8b - 4a - 4c$  if  $a \leq c + d$ . In particular,  $P(a, b, c)$  is always even. We call  $P(a, b, c)$  the *perimeter* of our six graphs  $A_{a,b,c}^{(i)}$ 's and  $F_{a,b,c}^{(i)}$ 's.

We need to show that

$$M(A_{a,b,c}^{(i)}) = \Phi_i(a, b, c) \text{ and } M(F_{a,b,c}^{(i)}) = \Psi_i(a, b, c), \quad (5.1)$$

for  $i = 1, 2, 3$ , by induction of the value the perimeter  $P(a, b, c)$  of the six graphs.

For the base cases, one can verify easily (5.1) with the help of `vaxmacs`, a software written by David Wilson<sup>3</sup>, for all the triples  $(a, b, c)$  satisfying *at least one* of the following conditions:

- (i)  $P(a, b, c) \leq 14$ ;
- (ii)  $b \leq 4$ ;
- (iii)  $c + d = 2b - a - c \leq 2$ .

For the induction step, we assume that (5.1) holds for all graphs  $A_{a,b,c}^{(i)}$ 's and  $F_{a,b,c}^{(i)}$ 's having perimeter  $P(a, b, c)$  less than  $p$ , for some  $p \geq 16$ . We will prove (5.1) for all  $A$ - and  $F$ -graphs with perimeter  $p$ .

By the base cases, we only need to show (5.1) for all graphs having the triple  $(a, b, c)$  in the following domain

$$\mathcal{D} := \{(a, b, c) \in \mathbb{Z}^3 : P(a, b, c) = p, b \geq 5, c + d \geq 3, d \geq 0, e \geq 0\}. \quad (5.2)$$

First, we partition  $\mathcal{D}$  into four subdomains as follows

$$\mathcal{D}_1 := \mathcal{D} \cap \{2 \leq a \leq c + d\},$$

$$\mathcal{D}_2 := \mathcal{D} \cap \{a \leq 1\},$$

$$\mathcal{D}_3 := \mathcal{D} \cap \{a > c + d, e \geq d\},$$

and

$$\mathcal{D}_4 := \mathcal{D} \cap \{a > c + d, e < d\}.$$

Next, we verify that (5.1) holds in each of the above subdomains.

---

<sup>3</sup>The software can be downloaded on the link <http://dbwilson.com/vaxmacs/>.

First, we consider the case  $(a, b, c) \in \mathcal{D}_1$ . We divide further  $\mathcal{D}_1$  into four subdomains (not necessarily disjoint) by:

$$\mathcal{D}_{1a} := \mathcal{D}_1 \cap \{d \geq 2, c \geq 1\},$$

$$\mathcal{D}_{1b} := \mathcal{D}_1 \cap \{d \geq 2, c = 0\},$$

$$\mathcal{D}_{1c} := \mathcal{D}_1 \cap \{d \geq 1, c \geq 2\},$$

and

$$\mathcal{D}_{1d} := \mathcal{D}_1 \cap \{d = 0, c \geq 2\}.$$

If  $(a, b, c) \in \mathcal{D}_{1a}$ , then  $P(a - 2, b - 2, c) = p - 8$ ,  $P(a - 1, b - 1, c) = P(a, b, c + 1) = P(a - 2, b - 2, c - 1) = p - 4$ . Thus, by induction hypothesis, we have for  $i = 1, 2, 3$

$$M(A_{a-2, b-2, c}^{(i)}) = \Phi_i(a - 2, b - 2, c), \quad (5.3)$$

$$M(A_{a-1, b-1, c}^{(i)}) = \Phi_i(a - 1, b - 1, c), \quad (5.4)$$

$$M(A_{a, b, c+1}^{(i)}) = \Phi_i(a, b, c + 1), \quad (5.5)$$

$$M(A_{a-2, b-2, c-1}^{(i)}) = \Phi_i(a - 2, b - 2, c - 1), \quad (5.6)$$

$$M(F_{a-2, b-2, c}^{(i)}) = \Psi_i(a - 2, b - 2, c), \quad (5.7)$$

$$M(F_{a-1, b-1, c}^{(i)}) = \Psi_i(a - 1, b - 1, c), \quad (5.8)$$

$$M(F_{a, b, c+1}^{(i)}) = \Psi_i(a, b, c + 1), \quad (5.9)$$

and

$$M(F_{a-2, b-2, c-1}^{(i)}) = \Psi_i(a - 2, b - 2, c - 1). \quad (5.10)$$

On the other hand, by Lemmas 3.3 and 4.2(a), we have  $M(A_{a, b, c}^{(i)})$ ,  $M(F_{a, b, c}^{(i)})$ ,  $\Phi_i(a, b, c)$ , and  $\Psi_i(a, b, c)$  all satisfy the recurrence (R2), for  $i = 1, 2, 3$ . Therefore, by the above equalities (5.3)–(5.10), we get  $M(A_{a, b, c}^{(i)}) = \Phi_i(a, b, c)$  and  $M(F_{a, b, c}^{(i)}) = \Psi_i(a, b, c)$ , for  $i = 1, 2, 3$ .

Similarly, if  $(a, b, c) \in \mathcal{D}_{1b}$ ,  $\mathcal{D}_{1c}$ , or  $\mathcal{D}_{1d}$ , we get (5.1) by using the recurrences (R3) and (R6) (see Lemmas 3.3(b) and 4.2(b)), (R4) (see Lemmas 3.4(a) and 4.3(a)), or (R5) (see Lemmas 3.4(b) and 4.3(b)), respectively. This implies that (5.1) holds for any triples  $(a, b, c) \in \mathcal{D}_1$ .

Next, we consider the case  $(a, b, c) \in \mathcal{D}_2$  (i.e. we are assuming  $a < c + d$ ). We reflect the graph  $A_{a, b, c}^{(i)}$  about a vertical line, and get the graph  $F_{f, e, d}^{(4-i)}$ , for  $i = 1, 2, 3$ . Similarly, we get graph  $A_{f, e, d}^{(4-i)}$  by reflecting the graph  $F_{a, b, c}^{(i)}$  about a vertical line. This means that

$$M(A_{a, b, c}^{(i)}) = M(F_{f, e, d}^{(4-i)}) \text{ and } M(F_{a, b, c}^{(i)}) = M(A_{f, e, d}^{(4-i)}), \quad (5.11)$$

for  $i = 1, 2, 3$ . Moreover, we can verify from the definition of the functions  $\Phi_i(a, b, c)$  and  $\Psi_i(a, b, c)$  that

$$\Phi_i(a, b, c) = \Psi_{4-i}(f, e, d) \text{ and } \Psi_i(a, b, c) = \Phi_{4-i}(f, e, d), \quad (5.12)$$

for  $i = 1, 2, 3$ . By (5.11) and (5.12), we only need to show that

$$M(A_{f,e,d}^{(i)}) = \Phi_i(f, e, d) \text{ and } M(F_{f,e,d}^{(i)}) = \Psi_i(f, e, d), \quad (5.13)$$

then (5.1) follows.

If  $e \leq 4$ , then the triple  $(f, e, d)$  satisfy the condition (ii) in the base cases, thus (5.13) follows. Then we can assume that  $e \geq 5$ . We now need to verify that the triple  $(f, e, d)$  is in the domain  $\mathcal{D}_1$ . It is more convenient to re-write the domain  $\mathcal{D}_1$  with all constraints in terms of  $a, b, c$  as follows:

$$\begin{aligned} \mathcal{D}_1 = \{(a, b, c) \in \mathbb{Z}^3 : & P(a, b, c) = p; 2 \leq a \leq 2b - a - c; b \geq 5; \\ & 2b - a - c \geq 3; 2b - a - 2c \geq 0; 3b - 2a - 2c \geq 0\}. \end{aligned} \quad (5.14)$$

We have in this case  $f = c + d - a \geq c + d - 1 \geq 2$  (we are assuming that  $a \leq 1$  and  $c + d \geq 3$ ). Moreover, the inequality  $f \leq 2e - f - d$  is equivalent to  $a \geq 0$ , so  $(f, e, d)$  satisfies the second constraint of the domain  $\mathcal{D}_1$ . This implies from the definition of the perimeter that  $P(f, e, d) = 8e - 4f - 4d = 8b - 4a - 4c = p$ . Next, the third constraint follows from our assumption  $e \geq 5$ . For the fourth constraint, we have  $2e - f - d = 2b - a - c = c + d \geq 3$ . Finally, we have  $2e - f - 2d = c \geq 0$  and  $3e - 2f - 2d = b \geq 0$ , which imply the last two constraints. Thus, the triple  $(f, e, d)$  is indeed in  $\mathcal{D}_1$ . By the case treated above, we have again (5.13). It means that (5.1) has just been verified for the case  $(a, b, c) \in \mathcal{D}_2$ .

The case  $(a, b, c) \in \mathcal{D}_3$  can be treated similarly to the case  $(a, b, c) \in \mathcal{D}_1$ . We also divide further  $\mathcal{D}_3$  into three subdomains:

$$\mathcal{D}_{3a} := \mathcal{D}_3 \cap \{c \geq 2\},$$

$$\mathcal{D}_{3b} := \mathcal{D}_3 \cap \{c = 1\},$$

and

$$\mathcal{D}_{3c} := \mathcal{D}_3 \cap \{c = 0\}.$$

If  $(a, b, c) \in \mathcal{D}_{3a}, \mathcal{D}_{3b}$ , or  $\mathcal{D}_{3c}$ , we use the recurrences (R1) (see Lemmas 3.2 and 4.1), (R2) (see Lemmas 3.3(a) and 4.2(a)), or (R3) and (R6) (see Lemmas 3.3(b) and 4.2(b)), respectively.

Finally, we consider the case  $(a, b, c) \in \mathcal{D}_4$  (i.e., we are assuming that  $a > c + d$ ). We also reflect the graphs  $A_{a,b,c}^{(i)}$ 's and  $F_{a,b,c}^{(i)}$ 's over a horizontal line, and get the reflection diagram as follows:

$$A_{a,b,c}^{(1)} \rightarrow A_{b,a,f}^{(1)},$$

$$A_{a,b,c}^{(2)} \rightarrow A_{b,a,f}^{(3)},$$

$$A_{a,b,c}^{(3)} \rightarrow A_{b,a,f}^{(2)},$$

$$F_{a,b,c}^{(1)} \rightarrow F_{b,a,f}^{(1)},$$

$$F_{a,b,c}^{(2)} \rightarrow F_{b,a,f}^{(3)},$$

$$F_{a,b,c}^{(3)} \rightarrow F_{b,a,f}^{(2)}.$$

Moreover, one readily gets from the definition of the functions  $\Phi_i(a, b, c)$  and  $\Psi_i(a, b, c)$  that

$$\begin{aligned}\Phi_1(a, b, c) &= \Phi_1(b, a, f), \\ \Phi_2(a, b, c) &= \Phi_3(b, a, f), \\ \Phi_3(a, b, c) &= \Phi_2(b, a, f), \\ \Psi_1(a, b, c) &= \Psi_1(b, a, f), \\ \Psi_2(a, b, c) &= \Psi_3(b, a, f),\end{aligned}$$

and

$$\Psi_3(a, b, c) = \Psi_2(b, a, f).$$

Therefore, we only need to verify that

$$M(A_{b,a,f}^{(i)}) = \Phi_i(b, a, f) \text{ and } M(F_{b,a,f}^{(i)}) = \Psi_i(b, a, f), \quad (5.15)$$

for  $i = 1, 2, 3$ , and (5.1) follows.

If  $a \leq 4$  or  $2a - b - f = b - c \leq 2$ , then  $(b, a, f)$  falls into one of the triples in our base cases, and (5.15) follows. Therefore we can assume that  $a \geq 4$  and  $b - c \geq 3$ . Similar to the case when  $(a, b, c) \in \mathcal{D}_2$ , if  $c \geq 1$ , one readily verifies that  $(b, a, f) \in \mathcal{D}_3$ ; and if  $c = 0$ , it is easy to see that  $(b, a, f) \in \mathcal{D}_1$ . Then, by the cases treated above, we obtain also (5.15).  $\square$

## 6 Proofs of Theorems 1.1 and 1.3

Before going to the proofs of Theorems 1.1 and 1.3, we quote the following useful lemma that was first introduced in [12] (see Lemma 3.6(a)).

**Lemma 6.1** (Graph Splitting Lemma). *Let  $G$  be a bipartite graph, and let  $V_1$  and  $V_2$  be the two vertex classes.*

*Assume that an induced subgraph  $H$  of  $G$  satisfies following two conditions:*

(i) (Separating Condition) *There are no edges of  $G$  connecting a vertex in  $V(H) \cap V_1$  and a vertex in  $V(G - H)$ .*

(ii) (Balancing Condition)  $|V(H) \cap V_1| = |V(H) \cap V_2|$ .

*Then*

$$M(G) = M(H) M(G - H). \quad (6.1)$$

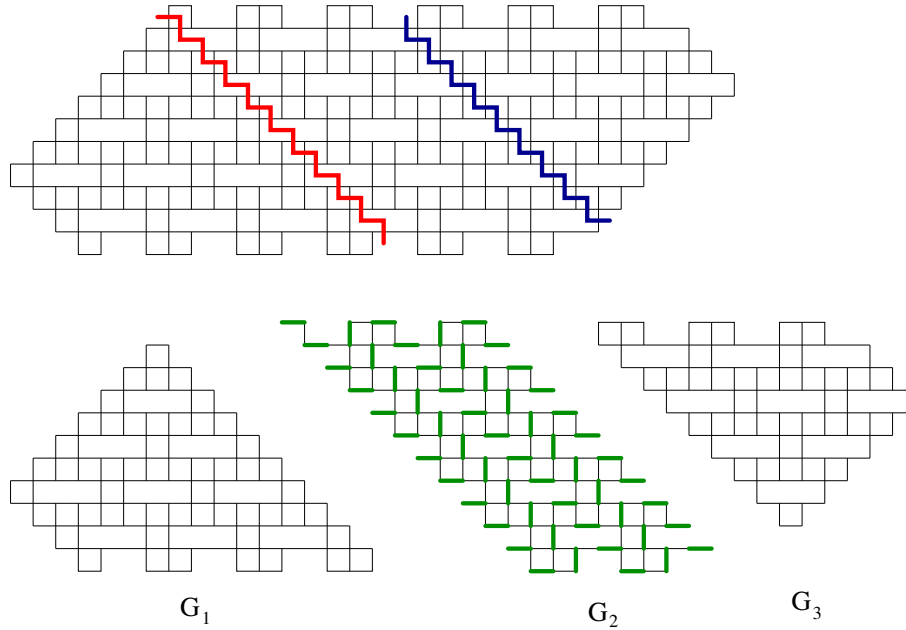


Figure 6.1: Illustrating the proof of Theorem 1.1.

*Proof of Theorem 1.1.* We split the graph  $TR_{a,b}$  into three subgraphs  $G_1$ ,  $G_2$  and  $G_3$  by two zigzag cuts as in Figure 6.1, for  $a = 2$  and  $b = 6$ . One readily sees that  $G_1$  satisfies the conditions in Graph-splitting Lemma 6.1 as an induced subgraph of  $G$ , and  $G_2$  in turn satisfies the conditions of the lemma as an induced subgraph of  $G - G_1$ . Therefore, we obtain

$$M(TR_{a,b}) = M(G_1) M(G - G_1) = M(G_1) M(G_2) M(G_3). \quad (6.2)$$

It is easy to see that  $G_2$  has a unique perfect matching (see the bold edges in Figure 6.1), and the graph  $G_1$  and  $G_2$  are isomorphic to  $A_{2a,3a,2a}^{(3)}$  and  $F_{2a,3a,2a}^{(1)}$ , respectively. By Theorem 2.1, we obtain

$$\begin{aligned} M(G_{a,2a,b}) &= M(A_{2a,3a,2a}^{(3)}) M(F_{2a,3a,2a}^{(3)}) \\ &= 2^{g(2a,3a,2a-1)+g(2a,3a,2a+1)} 5^{2g(2a,3a,2a)} 11^{2q(2a,3a,2a)} \\ &= 2^{a(a+1)+a(a-1)} 5^{2a^2} 11^{2\lfloor \frac{a^2}{4} \rfloor} \\ &= 10^{2a^2} 11^{\lfloor \frac{a^2}{2} \rfloor}, \end{aligned} \quad (6.3)$$

then the theorem follows.  $\square$

*Proof of Theorem 1.3.* The proof is illustrated in Figure 6.2, for  $m = 5$ ,  $n = 7$ ,  $h_1 = 4$  and  $h_2 = 3$ . Consider the rightmost subgraph  $G_1$  of  $TA_{m,n}^{h_1,h_2}$ , which is restricted by a dotted contour in Figure 6.2. By Graph Splitting Lemma 6.1, we obtain

$$M(TA_{m,n}^{h_1,h_2}) = M(TA_{m,n}^{h_1,h_2} - G_1) M(G_1). \quad (6.4)$$

Next, we consider the graph  $G'$  obtained from  $TA_{m,n}^{h_1,h_2} - G_1$  by removing horizontal forced edges (the circled ones on the right of  $G_1$  in Figure 6.2). Applying Graph-splitting Lemma 6.1 again to the second subgraph  $G_2$  of  $TA_{m,n}^{h_1,h_2}$ , which is restricted by a dotted contour, we have

$$M(G') = M(G' - G_2) M(G_2). \quad (6.5)$$

Repeat  $i := \lfloor \frac{h_1+1}{2} \rfloor - 2$  more times the above process, we get a graph  $\overline{G}$  and

$$M(TA_{m,n}^{h_1,h_2}) = M(\overline{G}) \prod_{j=1}^i M(G_j). \quad (6.6)$$

Apply the same process for the lower part of  $G$ . We get a graph  $\overline{\overline{G}}$  (the subgraph restricted by the bold contour in Figure 6.2) and

$$M(\overline{\overline{G}}) = M(\overline{G}) \prod_{j=1}^k M(H_j), \quad (6.7)$$

where  $k = \lfloor \frac{h_2+1}{2} \rfloor$ , and  $H_j$  is the  $j$ -th subgraph (*from the left*) restricted by a dotted contour in the lower part of  $G$ .

Combining (6.6) and (6.7), we deduce

$$M(TA_{m,n,h_1,h_2}^{(1)}) = M(\overline{\overline{G}}) \prod_{j=1}^i M(G_j) \prod_{j=1}^k M(H_j). \quad (6.8)$$

It is easy to see that  $M(G_j) = 1$  if  $h_1$  is odd, and 3 if  $h_1$  is even, for any  $j = 1, 2, \dots, i$ . Similarly,  $M(H_j) = 1$  if  $h_2$  is odd, and 3 if  $h_2$  is even, for any  $j = 1, 2, \dots, k$ . Thus,

$$M(TA_{m,n}^{h_1,h_2}) = 3^{\tau(h_1,h_2)} M(\overline{\overline{G}}). \quad (6.9)$$

On the other hand,  $\overline{\overline{G}}$  is isomorphic to the graph  $A_{a,b,c}^{(1)}$ , where  $a = n - \lfloor \frac{h_2+1}{2} \rfloor + 1$ ,  $b = m - \lfloor \frac{h_2+1}{2} \rfloor + 1$  and  $c = \lfloor \frac{h_1+1}{2} \rfloor$ . By (6.9) and Theorem 2.1, the equality (1.6) follows.

The equality (1.7) can be proved analogously.  $\square$

Next, we consider a variation of Theorem 1.3 as follows. Instead of using horizontal trimming lines as in Theorem 1.3, we consider two new stair-shaped trimming lines. The structure of each level in the new trimming lines is similar to the old ones (i.e. is a zigzag line with alternatively bumps and holes of size 2), and each two consecutive levels are connected by a "staircase" (see Figure 6.3). Assume that  $h_1$  is the distance between the top of the Aztec rectangle and the highest level of the upper trimming line, and  $h_2$  is the distance between the bottom of the Aztec rectangle and the lowest level of the lower trimming line. Again, by Graph Splitting Lemma 6.1(a), we can cut off small subgraphs with the same structure as that of  $G_i$  and  $H_j$ . We get again the final graph isomorphic to the graph  $A_{a,b,c}^{(1)}$ , with  $a, b, c$  defined as in the proof of Theorem 1.3 (see Figure 6.4). Therefore, we have the following result.

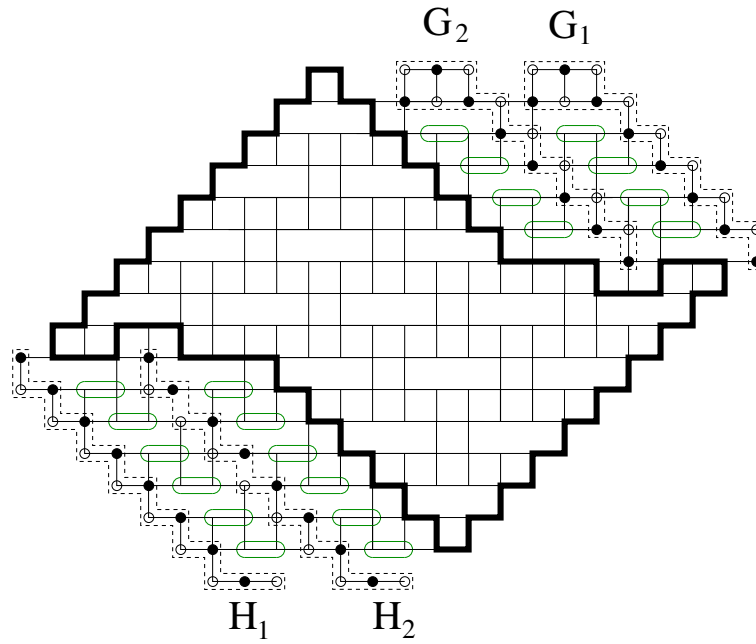


Figure 6.2: Illustrating the proof of Theorem 1.3.

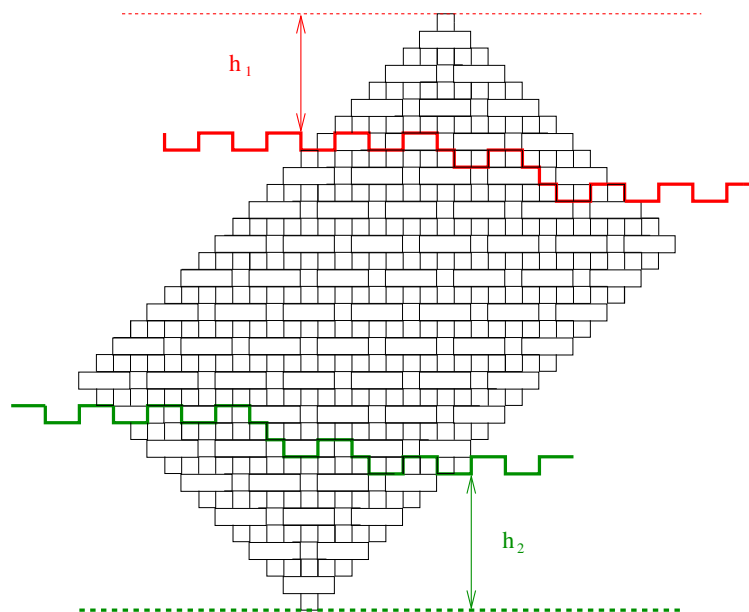


Figure 6.3:

**Theorem 6.2.** *Assume that  $\lfloor \frac{h_1+1}{2} \rfloor + \lfloor \frac{h_2+1}{2} \rfloor = 2(n - m)$ . Then the number of perfect matchings of the Aztec rectangle trimmed by two stair-shaped lines has all of its prime factors less than or equal to 13.*

The work of finding the explicit formulas for the numbers of perfect matchings (as

well as the precise definition of the new trimmed Aztec rectangle) in Theorem 6.2 will be left as an exercise.

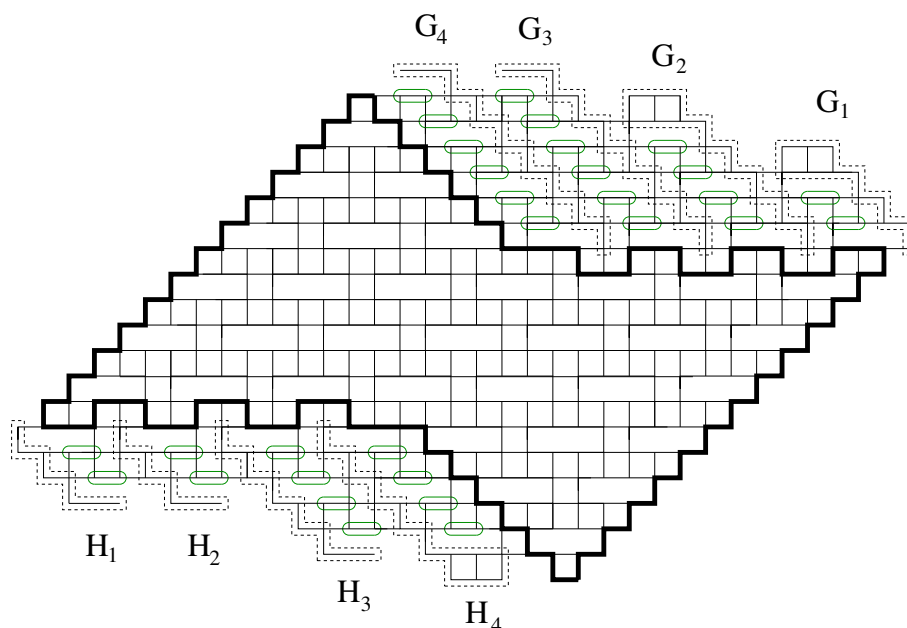


Figure 6.4: Illustrating the proof of Theorem 6.2.

## 7 Relation between the graph $TR_{a,b}$ and Hexagonal Dungeons

We consider the hexagonal dungeon  $HD_{a,2a,b}$  introduced by Blum [23] (see detailed definition of the hexagonal dungeon in [5]). Figure 7.1 shows the hexagonal dungeon  $HD_{2,4,6}$ . We consider the dual graph of  $HD_{a,2a,b}$  (i.e. the graph whose vertices are the small right triangles in  $HD_{a,2a,b}$  and whose edges connect precisely two triangles sharing an edge), which is denoted by  $G_{a,2a,b}$ . The upper graph with solid edges in Figure 7.3 illustrates the dual graph of  $HD_{2,4,6}$ . It has been proven by Ciucu and the author in [5] that the number of perfect matchings of  $G_{a,2a,b}$  is given by  $13^{2a^2} 14^{\lfloor \frac{a^2}{2} \rfloor}$ , which is similar to the number of perfect matchings of  $TR_{a,b}$  ( $10^{2a^2} 11^{\lfloor \frac{a^2}{2} \rfloor}$ ). This suggests the existence of a hidden connection between  $TR_{a,b}$  and the dual graph  $G_{a,2a,b}$  of the hexagonal dungeon.

If we assign some weights to the edges of a graph  $G$ , then we use the notation  $M(G)$  for the sum of weights of the perfect matchings of  $G$ , where the weight of a perfect matching is the product of weights of its constituent edges. We call  $M(G)$  the *matching generating function* of the weighted graph  $G$ .

Next, we quote a well-known subgraph replacement trick called *urban renewal*, which was first discovered by Kuperberg, and its variations found by Ciucu [1].

**Lemma 7.1** (Urban renewal). *Let  $G$  be a weighted graph. Assume that  $G$  has a subgraph  $K$  as one of the graphs on the left column in Figure 7.2, where only white vertices can*

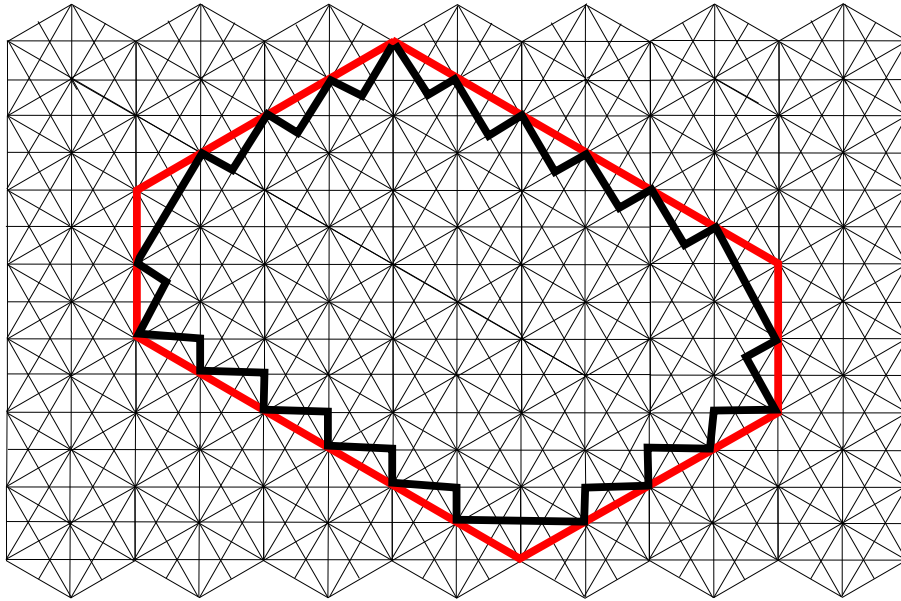


Figure 7.1: The hexagonal dungeon of sides 2, 4, 6, 2, 4, 6 (in cyclic order, starting from the western side). This Figure first appeared in [5].

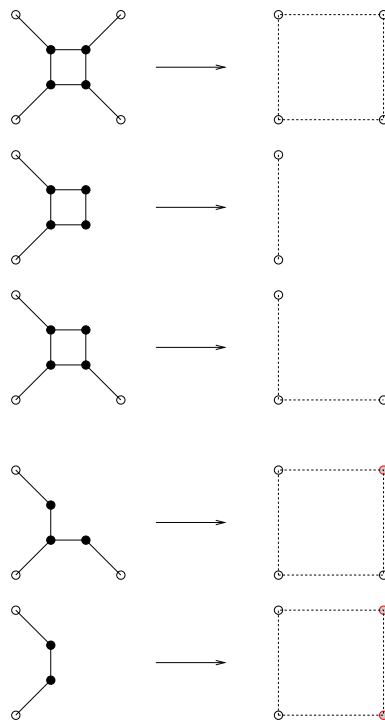


Figure 7.2: Urban renewal trick.

have neighbors outside  $K$ , and where all edges have weight 1. Let  $G'$  be the weighted graph obtained from  $G$  by replacing  $K$  by its corresponding graph  $K'$  on the right column

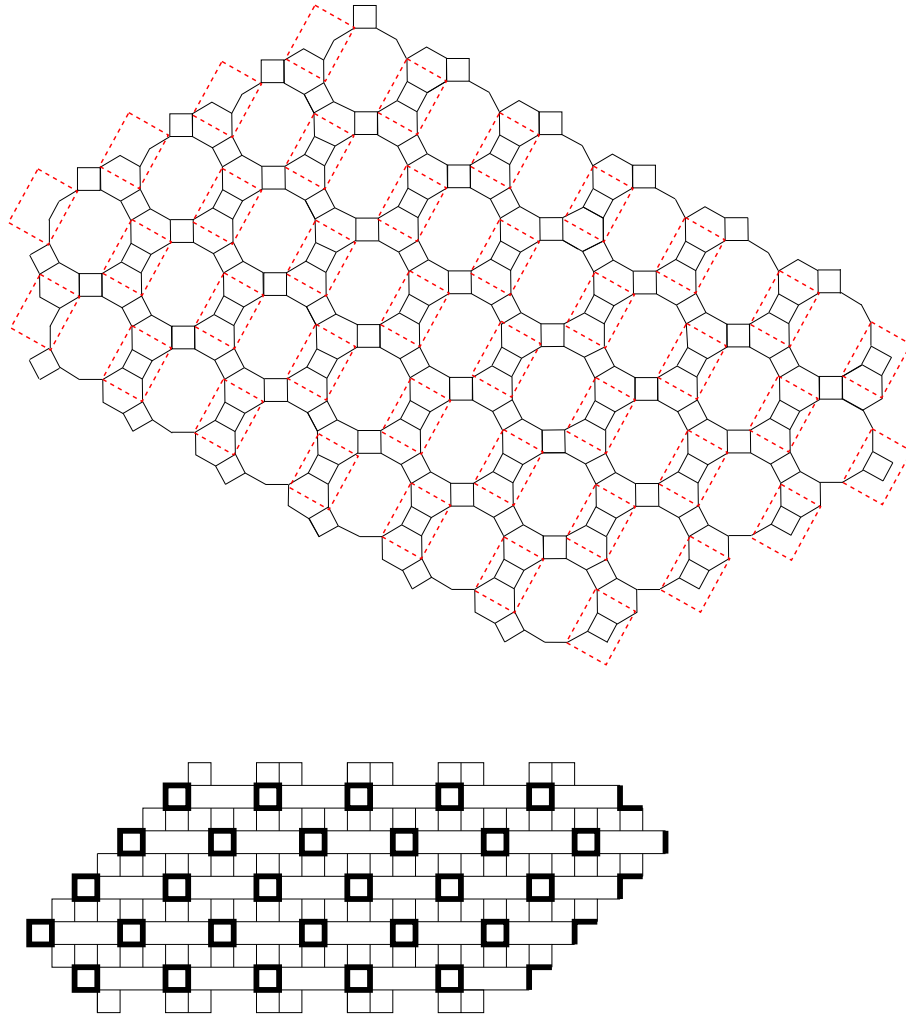


Figure 7.3: Deforming the dual graph of  $HD_{2,4,6}$  into a weighted graph on the square grid.

of Figure 7.2, where all dotted edges have weight  $\frac{1}{2}$ , and where the shaded vertices are the new ones which were not in  $G$ . Then we always have  $M(G) = 2M(G')$ .

Next, we apply suitable replacement rules in Lemma 7.1 to  $G_{a,2a,b}$  around the dotted rectangles as in the upper graph in Figure 7.3). Then we deform the resulting graph into a weighted graph  $\overline{G}_{a,2a,b}$  on the square lattice (see the lower graph in Figure 7.3; the bold edges have weight  $\frac{1}{2}$ ). We want to emphasize that even though the graphs  $\overline{G}_{a,2a,b}$  and  $TR_{a,b}$  have the same shape, their weight assignments are *different*. This means that Theorem 1.1 can *not* be deduced from the work in [5], and vice versa.

We now want to consider a common generalization of the weight assignments in the graphs  $\overline{G}_{a,2a,b}$  and  $TR_{a,b}$  as follows. Assume that  $x, y, z$  are three indeterminate weights. We assign weights to edges of the lattice  $B$  so that each cross pattern is weighted as in Figure 7.4. Denote by  $A_{a,b,c}^{(i)}(x, y, z)$ 's and  $F_{a,b,c}^{(i)}(x, y, z)$ 's the corresponding weighted

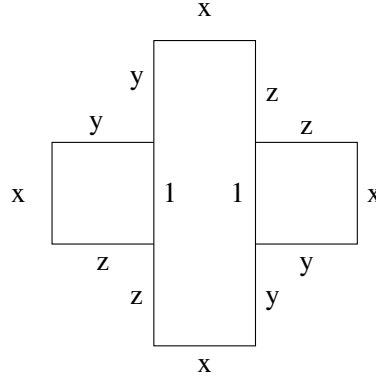


Figure 7.4: The weight assignment for each cross pattern.

versions of the graphs  $A_{a,b,c}^{(i)}$ 's and  $F_{a,b,c}^{(i)}$ 's, for  $i = 1, 2, 3$ , respectively.

Define the weighted versions of the functions  $\alpha(a, b, c)$  and  $\beta(a, b, c)$  by

$$\alpha(a, b, c; x, y, z) = \begin{cases} \frac{(x+2yz)yz}{x^2} & \text{if } 3b + a - c \equiv 5 \pmod{6}; \\ \frac{yz}{x} & \text{if } 3b + a - c \equiv 3 \pmod{6}; \\ \frac{x+yz}{x} & \text{if } 3b + a - c \equiv 1 \pmod{6}; \\ 1 & \text{otherwise} \end{cases} \quad (7.1)$$

and

$$\beta(a, b, c; x, y, z) = \begin{cases} \frac{(x+2yz)}{yz} & \text{if } 3b + a - c \equiv 1 \pmod{6}; \\ \frac{x}{yz} & \text{if } 3b + a - c \equiv 3 \pmod{6}; \\ \frac{(x+yz)x}{y^2z^2} & \text{if } 3b + a - c \equiv 5 \pmod{6}; \\ 1 & \text{otherwise.} \end{cases} \quad (7.2)$$

Our data suggests that

**Conjecture 7.2.** *The matching generating functions of the weighted graphs  $A_{a,b,c}^{(i)}(x, y, z)$ 's all have form*

$$\alpha(a, b, c; x, y, z) 2^X (x^2 + 2xyz + 2y^2z^2)^Y (2x^2 + 5xyz + 4y^2z^2)^Z x^T y^Q z^K, \quad (7.3)$$

for some  $X, Y, Z, T, Q, K$  depending on only  $a, b, c$ . Similarly, the matching generating functions of  $F_{a,b,c}^{(i)}(x, y, z)$ 's all have form

$$\beta(a, b, c; x, y, z) 2^{X'} (x^2 + 2xyz + 2y^2z^2)^{Y'} (2x^2 + 5xyz + 4y^2z^2)^{Z'} x^{T'} y^{Q'} z^{K'}, \quad (7.4)$$

for some  $X', Y', Z', T', Q', K'$  depending on only  $a, b, c$ .

Denote by  $TR_{a,b}(x, y, z)$  the corresponding weighted version of the graph  $TR_{a,b}$ . If Conjecture 7.2 is true, then by the graph-splitting trick in the proof of Theorem 1.1, we can implies that the matching generating function of  $TR_{a,b}(x, y, z)$  is also given by powers of  $2, x, y, z, (x^2 + 2xyz + 2y^2z^2)$ , and  $(2x^2 + 5xyz + 4y^2z^2)$ .

## Acknowledgements

This research was supported in part by the Institute for Mathematics and its Applications with funds provided by the National Science Foundation (grant no. DMS-0931945).

## References

- [1] M. Ciucu. Perfect matchings and perfect powers. *J. Algebraic Combin.* **17**: 335–375, 2003.
- [2] M. Ciucu. Aztec dungeons and powers of 13. *Combinatorics Seminar*, Georgia Institute of Technology, October 2000.
- [3] M. Ciucu. Another dual of MacMahon’s theorem on plane partitions. *Adv. Math.* **306**: 427–450, 2017.
- [4] M. Ciucu and I. Fischer. Lozenge tilings of hexagons with arbitrary dents. *Adv. App. Math.* **73**: 1–22, 2016.
- [5] M. Ciucu and T. Lai. Proof of Blum’s Conjecture on Hexagonal Dungeons. *J. Combin. Theory Ser. A* **125**: 273–305, 2014.
- [6] N. Elkies, G. Kuperberg, M. Larsen, and J. Propp. Alternating-sign matrices and domino tilings (Part I). *J. Algebraic Combin.* **1**: 111–132, 1992.
- [7] N. Elkies, G. Kuperberg, M. Larsen, and J. Propp. Alternating-sign matrices and domino tilings (Part II). *J. Algebraic Combin.* **1**: 219–234, 1992.
- [8] P. W. Kasteleyn. The statistics of dimers on a lattice: I. The number of dimer arrangements on a quadratic lattice. *Physica* **27**(12): 1209–1225, 1961.
- [9] E. H. Kuo. Applications of Graphical Condensation for Enumerating Matchings and Tilings. *Theor. Comput. Sci.* **319**: 29–57, 2004.
- [10] P. A. MacMahon. *Combinatory Analysis*, vol. 2. *Cambridge Univ. Press*, 1916, reprinted by *Chelsea*, New York, 1960.
- [11] T. Muir. *The Theory of Determinants in the Historical Order of Development*, vol. I. *Macmillan*, London, 1906.
- [12] T. Lai. Enumeration of hybrid domino-lozenge tilings. *J. Combin. Theory Ser. A* **122** 53–81: 2014.
- [13] T. Lai. New aspects of regions whose tilings are enumerated by perfect powers. *Elec. J. of Combin.* **20**(4): #P31, 2013.
- [14] T. Lai. A generalization of Aztec dragons. *Graph Combin.* **2**(5): 1979–1999, 2016.
- [15] T. Lai. A new proof for the number of lozenge tilings of quartered hexagons. *Discrete Math.* **338**: 1866–1872, 2015.
- [16] T. Lai. Proof of a conjecture of Kenyon and Wilson on semicontiguous minors. *ArXiv Mathematics e-prints*, July 2015. [arXiv:1507.02611](https://arxiv.org/abs/1507.02611).
- [17] T. Lai. A  $q$ -enumeration of lozenge tilings of a hexagon with three dents. *Adv. Appl. Math.* **82**: 23–57, 2017.

- [18] T. Lai. A  $q$ -enumeration of lozenge tilings of a hexagon with four adjacent triangles removed from the boundary. *European J. Combin.*, **64**:66–87, 2017.
- [19] T. Lai. Lozenge tilings of a halved hexagon with an array of triangles removed from the boundary. *ArXiv Mathematics e-prints*, October 2016. [arXiv:1610.06284](https://arxiv.org/abs/1610.06284) .
- [20] T. Lai. Lozenge Tilings of a Halved Hexagon with an Array of Triangles Removed from the Boundary, Part II. *ArXiv Mathematics e-prints*, September 2017. [arXiv:1709.02071](https://arxiv.org/abs/1709.02071).
- [21] T. Lai and G. Musiker. Beyond Aztec castles: Toric cascades in the dP3 quiver. To appear in *Comm. Math. Phys.* 2017. DOI: 10.1007/s00220-017-2993-8.
- [22] T. Lai and R. Rohatgi. Cyclically Symmetric Tilings of a Hexagon with Four Holes. Submitted for publication. *ArXiv Mathematics e-prints*, May 2017. [arXiv:1705.01122](https://arxiv.org/abs/1705.01122).
- [23] J. Propp. Enumeration of matchings: Problems and progress. *New Perspectives in Geometric Combinatorics. Cambridge Univ. Press*, 255–291, 1999.
- [24] R. Rohatgi. Enumeration of lozenge tilings of halved hexagons with a boundary defect. *Electron. J. Combin.* **22**(4), #P4.22, 2015.
- [25] R. Rohatgi. Enumeration of tilings of a hexagon with a maximal staircase and a unit triangle removed. *Australas. J. Combin.* **65**(3): 220–231, 2016.
- [26] H. Sachs and H. Zernitz. Remark on the dimer problem. *Discrete Appl. Math.* **51**: 171–179, 1994.
- [27] M. Saikia. Enumeration of Domino Tilings of an Aztec Rectangle with boundary defects. *Adv. App. Math.* **89**: 41–66, 2017.
- [28] R. Stanley. Enumerative combinatorics, Vol 2. *Cambridge Univ. Press*, 1999.
- [29] H. N. V. Temperley and M. E. Fisher. Dimer problem in statistical mechanics- an exact result. *Phil. Mag.* **6**: 1061–1063, 1961.
- [30] B.-Y. Yang. Two enumeration problems about Aztec diamonds. Ph.D. thesis, Department of Mathematics, Massachusetts Institute of Technology, MA, 1991.